Project B.14 – Demonstration of Enhanced Fire Safety Technology – Fire Suppression Systems

Part 2A: Evaluation of Fire Suppression Systems in a Full Scale Vehicle Fire Test and Static Vehicle Fire Tests

Jeffrey Santrock
General Motors Corporation

and

Steven E. Hodges
Santa Barbara, California

Abstract

This report describes tests of a prototype fire suppression system installed in the engine compartment of a test vehicle. The prototype fire suppression system consisted of 2 Solid Propellant Gas Generators (SPGG) and two optical detectors. These components was installed on the hood of the test vehicle and powered from the battery in the test vehicle. The test vehicle was subjected to a crash test in which power steering fluid expelled onto the exhaust manifold autoignited. In this test, the prototype fire suppression system failed to extinguish this fire. A series of four static fire tests were conducted using the crash tested vehicle. For these static fire tests, the vehicle was stationary. Two fully charged SPGG units were installed in the test vehicle before each test. The first static fire test involved manual activation of the SPGG unite without a fire underhood. This was done to evaluate the effect of the SPGG discharge on underhood components. In the subsequent three static fire tests, fires were ignited in the engine compartment using an electrical igniter or by spraying power steering fluid onto a metal block heated by electrical heaters. In these static fire tests, the prototype fire suppression system failed to extinguish the test fire in two tests and extinguished the test fire in one test.

Table of Contents

Appendicies

List of Figures

Report

List of Figures

Appendicies

List of Tables

Report

1 Introduction

The tests described in this report were conducted by General Motors (GM) pursuant to an agreement between GM and the U.S. Department of Transportation. The purpose of these tests was to evaluate the effects of selected on-board fire suppression systems in fire tests of crash-tested vehicles. An experimental fire suppression system based on optical fire detection and Solid Propellant Gas Generator (SPGG) fire suppressant technology was installed in the engine compartment of a test vehicle (1999 Honda Accord). The test vehicle was then subjected to a crash test using a test protocol that resulted in a fire in the engine compartment of a similar test vehicle in a previous crash test [1]. The cause of the fire in the previous crash test was determined to be autoignition of power steering fluid expelled from the power steering fluid reservoir onto the exhaust manifold [1]. After this crash test, a series of static fire tests using the crash-tested vehicle were conducted where fires in the engine compartment were staged to further evaluate this system. Ignition scenarios used in these static fire tests included ignition of solid combustible materials using a resistively heated wire and autoignition of a combustible fluid sprayed onto a heated metal plate.

The criteria for assessing the effectiveness of the fire suppression system in the event of a fire during the crash test and during the subsequent fire tests were: (i) the fire suppression system remained functional during and after the crash test and (ii) the fire suppression system extinguished a fire in the engine compartment during the crash test or during staged fires in the subsequent static fire tests. The rational for selecting fire suppression systems based on SPGG technology for the tests described in this report is discussed in Section 3. The intent of using the crash tested vehicle in a series of static vehicle fire tests was to examine the performance of this type of fire suppression system under different fire scenarios in the engine compartment of a post-collision vehicle.

2 Crash Test

The crash test (C12610) occurred on August 10, 1999. The test vehicle was stationary and was struck in the left front by a moving barrier. The moving barrier had a deformable aluminum honeycomb face similar to that described in FMVSS 214. The target angle between the trajectory of the barrier and the longitudinal mid-line of the vehicle was approximately 21 $\pm$ 2 degrees, with the barrier trajectory intersecting the center of gravity of the test vehicle. The horizontal center-line of the barrier's simulated bumper was aligned with the horizontal center-line of the rear bumper beam in the test vehicle. The mass of the moving barrier was 1635.0 kg. The barrier speed at impact was 105.0 km/hr. The mass of the test vehicle was 1738.0 kg (966.0 kg front

and 772.0 kg rear).[1] The crash test setup is illustrated schematically in Figure 1. Figure 2 is a photograph of the test vehicle and barrier before this crash test showing the alignment of the vehicle relative to the barrier.

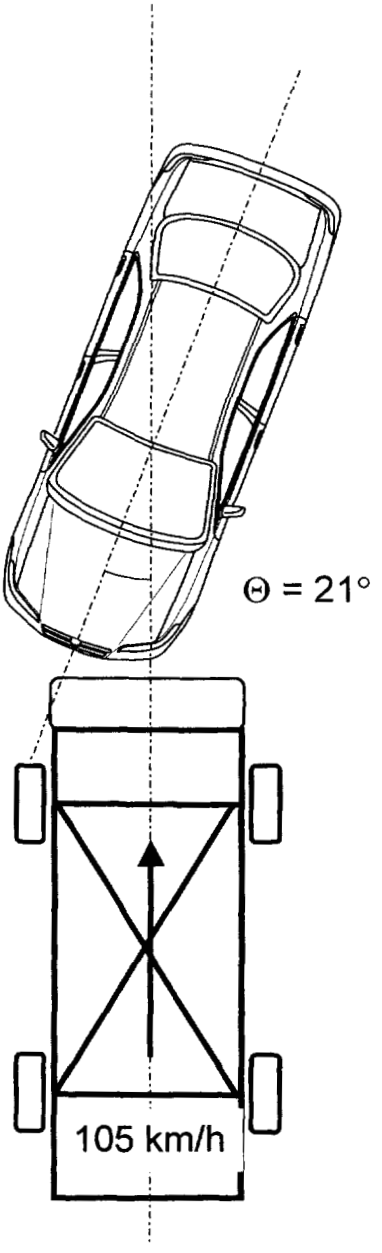

Figure 1. Crash test set-up for C12610.

[1] The test vehicle contained two 50th percentile adult male anthropomorphic body forms in the front seating positions for ballast. The mass of each ATD was 75.7 kg. No data were recorded from the anthropomorphic body forms during either test.

[2] The test vehicle contained two 50th percentile adult male anthropomorphic body forms in the front seating positions for ballast. The mass of each ATD was 75.7 kg. No data were recorded from the anthropomorphic body forms during either test.

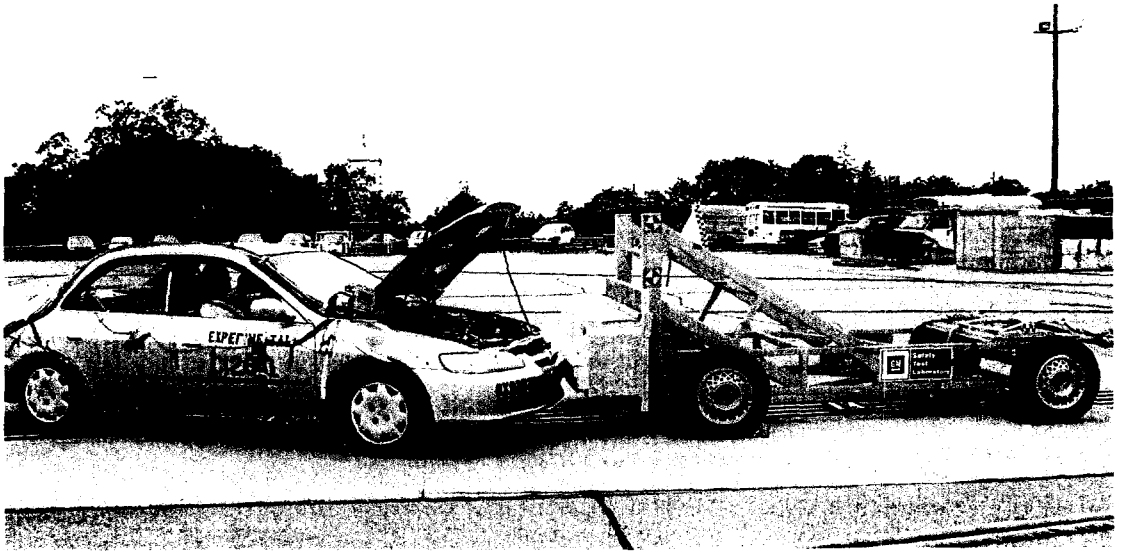

Figure 2. Crash Test C12610. Photograph of the test vehicle and barrier before this test showing the alignment of the vehicle.

The transmission was in neutral. The brakes were on. The air conditioning was on with the blower set on high. The Hi-beam headlights were on. The radio was on. The fire suppression system was active.

A static (vehicle stationary) engine warm-up procedure was used in these tests to achieve underhood temperatures greater than ambient for the test vehicle. The test vehicle contained the factory fills of motor oil (5.6 L), transmission fluid (6.2 L), engine coolant (6.9 L), brake fluid (capacity unknown), power steering fluid (1.1 L), and windshield washer fluid. The fuel tank in the test vehicle contained 61 L of Stoddard Solvent, which represents approximately 95% of the usable capacity of the fuel tank. Gasoline for the engine was supplied from a secondary fuel tank with a capacity of approximately 8 L mounted in the rear compartment area for these tests. The secondary fuel tank was fabricated from aluminum plate and fitted with a new service parts fuel pump for a 1999 Honda Accord. The wiring harness and fuel lines in the test vehicle were connected to the fuel pump in the secondary fuel tank. To achieve engine compartment temperatures representative of some driving conditions, a pre-impact warm-up schedule was followed in which the test vehicle was idled with an engine speed of 1500 to 1800 rpm for approximately 70 minutes before impact. At impact, the ignition in the test vehicle was on and the engine was running at approximately 1400 rpm; the transmission was in neutral; the brakes were on; the heater was on with the blower set on high; the Hi-beam headlights were on; and the radio was on. Figure 3 shows the crash test vehicle before and after this crash test.

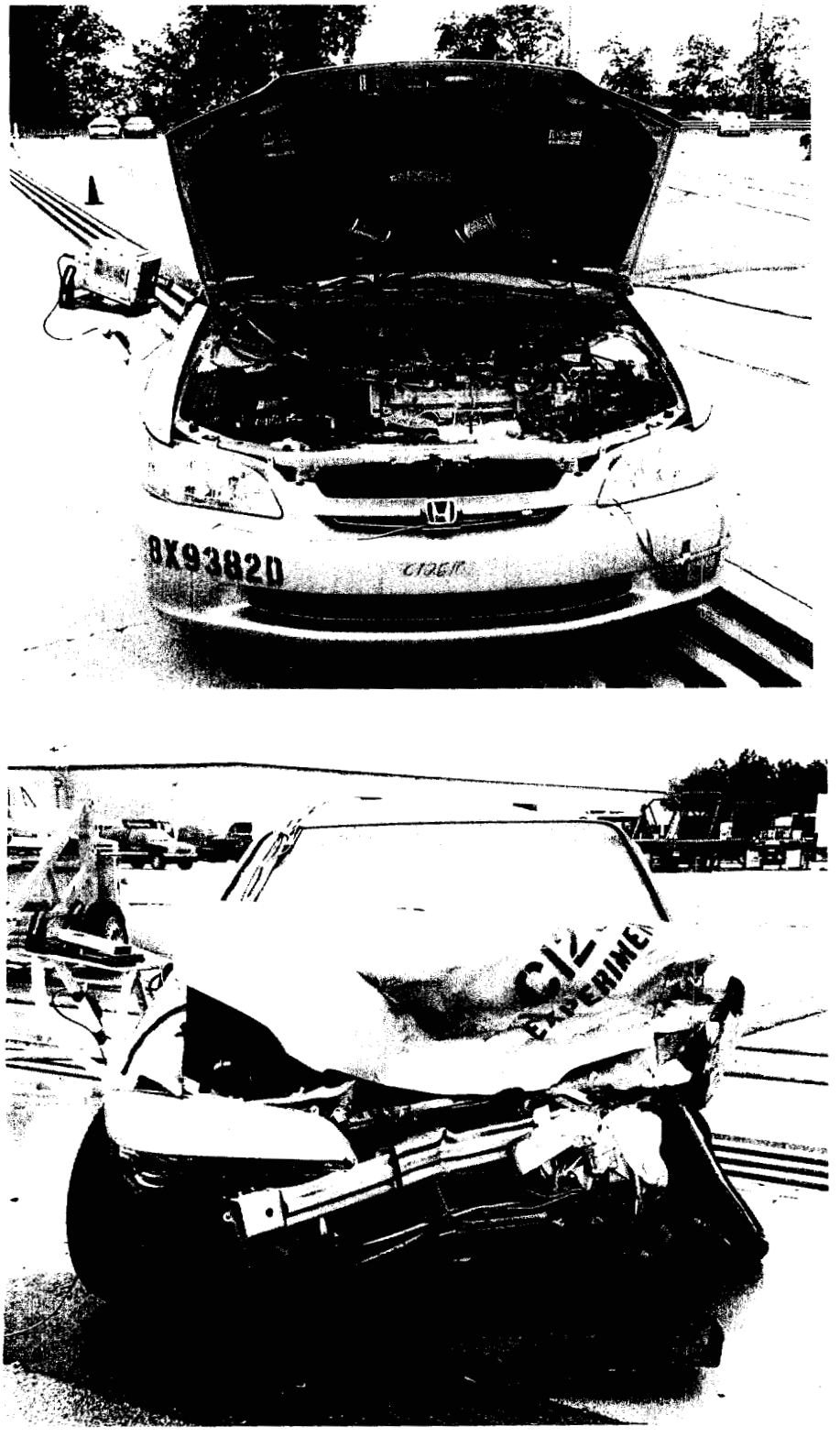

Figure 3. Crash Test C12610. Photographs of the test vehicle before (upper) and after (lower) this crash test.

2.1 Crash Test Summary

Data recorded from accelerometers located on the test vehicle's rocker panels are contained in Appendix A. Data recorded from the flammable vapor sensors are located in Appendix B. Gas chromatography data for gases found in the engine compartment are in Appendix C. Manifold voltage and temperature data as well as thermocouple temperature data can be found in Appendix D.

The test vehicle and crash test protocol used here were intended to reproduce a previous crash test in which a fire occurred in the engine compartment [1]. The cause of the fire in the previous crash test was determined to be autoignition of power steering fluid expelled from the power steering fluid reservoir onto the exhaust manifold [1].

A fire was observed during Crash Test C12610. The test data acquired during the crash test reported in the appendicies are consistent with the autoignition of power steering fluid on the exhaust manifold. Specifically:

- The GC / MS data from this crash test shows a small amount of gasoline vapor and a relatively large amount of power steering fluid aerosol / vapor at the exhaust manifold collector during the crash test (Appendix C, Plot C6).

- The surface temperature of the exhaust manifold collector (T3) at the time of impact during this crash test was approx. 400°C (Appendix D, Plot D3). Based on previous testing, this was sufficient to result in autoignition for Honda factory fill power steering fluid [1], and indicates that ignition occurred on the exhaust manifold runner near the oxygen sensor.

- The high speed film from the camera mounted on the right front fender showed a fire plume at the exhaust manifold starting at about 180 milliseconds after time zero.

Section 3.1 contains a more detailed analysis of the crash test data and of the performance of the fire suppression system in this crash test.

The SPGG units automatically discharged during this crash test. Figure 4 shows close-up views of the optical detectors and SPGG units on the hood before and after this crash test.

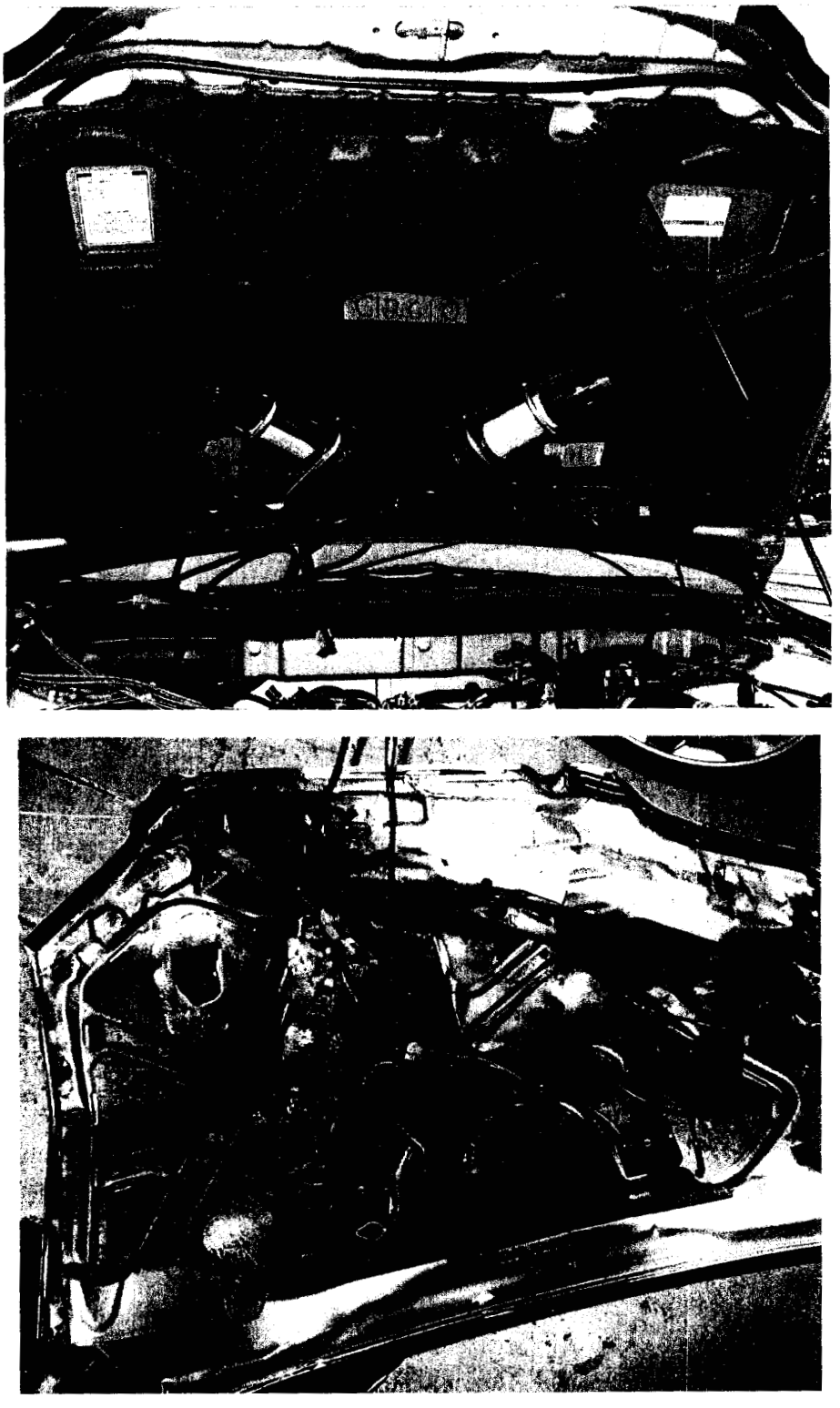

Figure 4. Crash Test C12610. Photographs of the optical detectors and SPGG units on the hood before (upper) and after (lower) this crash test.

2.1.1 Vehicle Warm-up Timing

Table 1 summarizes the pre-impact warm-up schedules for the test vehicle.

Table 1
Summary of Collision Test Countdown

Time (hr:min)	Action
0:00	Start Engine
0:03	Idle 1300-1500 rpm; Install SPGG Units Under Hood.
0:04	A/C – On; Low Beam Headlamps – On.
0:05	Radio – On
0:50	Connect SPGG Units to Optical Detectors. (1 Detector out of 4 Not Functioning)
0:53	Gas Sensor Electronics – Off
0:55	Begin Instrumentation Set-Up
0:57	End Instrumentation Set-Up
1:00	Gas Sensor Electronics – On; Gear to Neutral; Parking Brake – Off; Check Squib Continuity
1:00	Begin Countdown

2.1.2 Vehicle Mass, Barrier Mass, and Impact Parameters

The test vehicle's front, rear, and total mass, as well as the barrier's total mass, speed at the time of impact, and place of impact are summarized in Table 2.

Table 2
Test Vehicle Mass, Barrier Mass, Barrier Velocity, and Location of Impact

	Test Data
Vehicle Test Mass – Front	966.0 kg
Vehicle Test Mass – Rear	772.0 kg
Vehicle Test Mass – Total	1738.0 kg
Barrier Mass	1635.0 kg
Barrier Velocity at Impact	105.0 km/hr
Location of Impact	Frontal impact at test vehicle's left front corner, with a target angle of 21 ± 2° between the longitudinal midline of the vehicle and the trajectory of the barrier.

2.1.3 Accelerometer Data

Five tri-axial (longitudinal, lateral, and vertical) accelerometers were mounted to the test vehicle in the following locations: Right Front Rocker Panel; Left Front Rocker Panel; Right Rear Rocker Panel; Left Rear Rocker Panel; Hood Center. Each of these sensors recorded acceleration. The purpose of the accelerometer mounted to the hood was to help troubleshoot a fire suppression system failure if it occurred during the crash test. Note that the accelerometer on the hood was affected by (1) ringing of the hood, (2) rotation of the vehicle and accelerometer, (3) crush of the hood, and (4) chatter of the accelerometer on the hood. The accelerometers were glued and bolted to the inner hood panel, but the glue bond failed during the crash test, allowing the sensors to chatter. The highest magnitude acceleration was recorded at 20.0 ms. The second highest magnitude acceleration was recorded longitudinally at the Hood Center, at 19.5 ms

The change in velocity of the test vehicle was calculated from the recorded acceleration data. The maximum change in velocity of the vehicle recorded calculated from the accelerometer data was 57.6 km/h at 107.7 ms. The velocities calculated from the accelerometers located in the rear of the vehicle, away from the crush zone can be combined (root sum squared) to yield an estimate of the peak center of mass change in velocity, approximately 49 km/hr at 70 milliseconds after impact.

2.2 Flammable Vapor Sensors

Five flammable gas sensors (TGS 813, FIGARO USA, Inc, Wilmette, IL) were installed in the engine compartments of the test vehicle. Gas Sensor S1 was located to the right of the oxygen sensor in the exhaust manifold. Gas Sensor S2 was located at the upper right of the exhaust manifold heat shield. Gas Sensor S3 was located at the upper left of the exhaust manifold heat shield. Gas Sensor S4 was located above the left side of the fuel rail. Gas Sensor S5 was located above the right side of the fuel rail.

Gas phase concentration – sensor output voltage calibration data was obtained using heptane in the range of 0 to 5% (V/V). The tin oxide semiconductor elements in these sensors also respond to changes in temperature. Exposure to heated vapor or aerosol from fluids expelled during the crash test, to flame, or to the effluent from the solid propellant gas generators that activated during this test can cause the sensor output voltage to increase as if the sensor was exposed to a flammable gas. Interpretation of the flammable sensor data therefore must include consideration of the results of the gas chromatography / mass spectrometry analysis of gas samples acquired from these locations during the crash test shown in Appendix C and of the exposure of each sensor to flame and the SPGG effluent.

2.2.1 Flammable Vapor Data

The SPGG units activated at approximately 300 milliseconds after impact during this crash test. As the gas sensors in the engine compartment were exposed to the effluent from the SPGG units, which can affect the response of this type of detector, the gas concentration data shown in plots B1 through B5 in Appendix B is not a reliable measure of flammable gas concentration in the engine compartment of the test vehicle.

2.3 Gas Chromatography / Mass Spectroscopy Analysis of Engine Compartment Air Samples

Air samples were acquired from five locations in the engine compartments of the test vehicle during the crash test. The inlet of Sample Tube T1 was located in an opening in the exhaust manifold heat shield for the oxygen sensor. The inlet of Sample Tube T2 was located in the space between the top of the exhaust manifold and the exhaust manifold heat shield. The inlet of Sample Tube T3 was located on the upper surface of the exhaust manifold heat shield approximately above the inlet to Sample Tube T2. The inlet of Sample Tube T4 was located in

the center of the left side of the fuel rail. The inlet of Sample Tube T5 was located above the right side of the fuel rail.

2.3.1 Gas Chromatography / Mass Spectroscopy Analysis of Engine Compartment Air Sample Data

Gas chromatography/mass chromatography analyses of air sampled from the engine compartment during this crash test show the presence of windshield washer fluid (Methanol), gasoline vapor (Hydrocarbons – 1), brake fluid vapor / aerosol (Poly(Glycol) Ethers), power steering fluid vapor /aerosol (Hydrocarbons – 2), and engine coolant (Ethylene Glycol) [see Appendix C]. The gas chromatography / mass spectrometry analyses detected no organic vapors or aerosols near the oxygen sensor on the right side of the exhaust manifold collector (Location 1). The gas chromatography / mass spectrometry analyses showed hydrocarbons from gasoline (Hydrocarbons – 1) and from power steering fluid (Hydrocarbons – 2) above the exhaust manifold heat shield (Location 3) and above the exhaust manifold runners behind the exhaust manifold heat shield (Location 2). The gas chromatography / mass spectrometry analyses showed hydrocarbons from gasoline (Hydrocarbons – 1), poly(glycol) ethers from brake fluid, and hydrocarbons from power steering fluid (Hydrocarbons – 2) in air samples from above the fuel rail (Locations 4 and 5). Methanol from windshield washer fluid and ethylene glycol from engine coolant were detected in the air sample from above the right side of the fuel rail.

2.4 Component Temperatures

Thermocouples were mounted on the exhaust system to measure surface temperatures before and during the crash. The purpose was to measure exhaust system surface temperatures and determine whether autoignition temperatures were reached for various underhood fluids (e.g., motor, transmission fluid, power steering fluid, etc.), and to help determine the cause of a fire if one occurred in the engine compartment of the test during the crash test.

2.4.1 Component Temperature Data

Appendix D contains plots of data recorded from thermocouples during this crash test. Table 3 shows temperatures recorded from these thermocouples at the time of impact.

Exposure to heated gases in the effluent from the SPGG discharge appeared to have caused an increase of about 20°C in the air temperature in the engine compartment about 3 seconds after impact (Plot D4). Temperature data recorded after about 150 seconds post-impact were invalid because of the failure of test instrumentation in the engine compartment exposed to flames.

Table 3
Temperatures Recorded at Impact

Thermocouple / Location	Temperature
Thermocouple 1 Exhaust Manifold Runner No. 3	321°C
Thermocouple 2 Exhaust Manifold Runner No. 4	268°C
Thermocouple 3 Exhaust Manifold Collector	401°C
Thermocouple 4 Engine Compartment Air Temperature	92°C
Thermocouple 5 Exhaust Manifold Heat Shield Surface	81°C

2.5 Crash Test Fire Suppression System

The fire suppression system installed in the engine compartment of the test vehicle for this test included two prototype solid propellant gas generator fire suppression units (Atlantic Research Corporation, Knoxville, TN) and two prototype optical flame detectors (SRS Technologies, Huntsville, AL). The solid propellant gas generator flame suppression units were bolted to the lower surface of the hood using two U-blots for each unit. The optical flame detectors were attached to the lower surface of the hood using two through-bolts for each unit. Flame Suppression Unit 1 and Flame Detector 1 were attached to the left side of the hood rearward of the crush initiator in the inner hood panel. Flame Suppression Unit 2 and Flame Detector 2 were attached to the right side of the hood rearward of the crush initiator in the inner hood panel. See Figure 3.

3 Evaluation of the Selected SPGG Fire Suppression System

Fire suppression systems based on solid propellant gas generator technologies were selected for the tests described in this report based on (1) the results of testing conducted by the Building and Fire Research Laboratory, National Institutes of Standards and Technologies (BFRL/NIST) and (2) evaluation of system characteristics in proposals received from suppliers of fire suppression

systems that, in principle, could be adapted for use in motor vehicles. In a separate testing program, researchers at the BFRL / NIST evaluated a number of fire suppression technologies in small- and large-scale laboratory tests. These tests examined the effectiveness of gaseous fire suppression agents, dry chemical fire suppression agents, and SPGG fire suppression systems in a number of laboratory fire scenarios. The results of the BFRL/NIST testing program indicated the following order of effectiveness for the three types of technologies tested: SPGG systems > dry chemical agents > gaseous agents [2].

Fire Protection Systems designed to be integrated onto a vehicle have become commonplace for larger vehicles, such as transit buses [3]. Systems for smaller automobiles are not widely available. Proposals from four suppliers were evaluated to select a fire suppression system for the tests described in this report. Two of these proposals described fire suppression systems based on optical flame detectors and some type of dry chemical agent contained in one or more pressurized reservoir. Two proposals described fire suppression systems based on optical flame detectors and SPGG units. Dry chemical weight density flow rate concentrations (mass/protected volume/sec) of approximately 3 $kg/m^3/s$ (0.2 $lb/ft^3/s$) are required to suppress or extinguish a fire. This concentration must be maintained long enough so that reflash does not occur [4]. The required duration of the agent discharge will depend on application details, i.e., maximum delay between a fire alarm and the stoppage of air flow, time from collision to coming to rest, and so on [5]. The proper performance of dry chemical fire extinguishing systems depends critically on good design and correct system installation. Critical parameters include discharge nozzle quantity and location, agent distribution length, and, of course, amount of agent [6]. Discharge durations for onboard vehicle fire extinguishers range from 10 sec for small vehicles with protected volumes of less than about 1 m^3, to more than 30 sec for larger protected volumes.

Fire suppression systems based on SPPG technology use a solid propellant similar to that used in air bag inflators to produce a mixture of inert gases and particulate that is propelled onto the fire in a high velocity gas discharge. Fire suppression can occur as a result of one or a combination of four mechanisms [7]. The inert gases released from the SPGG units displace air and reduce the supply of oxygen to the flame. Expansion of the inert gases reduces the total energy and thus the temperature of the flame, the Joule–Kelvin effect [8]. The residue from the propellant forms an aerosol in the effluent from the SPGG and, depending on the chemistry of gas generation from the solid propellant, this residue may have fire suppression properties similar to dry chemical agents. Finally, the high velocity discharge of gases from the SPGG unit can result in separation of the flame from the fuel source.

The fire suppression system used in this test was tested as received from the supplier without modification. Technical personnel from General Motors installed the optical flame sensors, inert SPGG units, and cabling in the test vehicle following instructions supplied by the supplier. Just before each test described in this report, active SPGG units were installed in the test vehicle by technical personnel from the supplier. Technical personnel from the supplier performed a final systems check to ensure that the system was functioning within specifications before the test. Figure 3 shows the suppression system's mounting configuration within the crash test vehicle's engine compartment.

The active fire suppression system tested here consisted of two SPGG units and two optical flame sensors. A fire suppression system was installed in the engine compartment of the test vehicle and this vehicle was subjected to a frontal crash test. The system was configured so that detection of fire by one or both of the flame sensors would trigger the discharge of both SPGG units. Technical personnel from General Motors worked with the supplier to determine mounting locations for each component in the test vehicle to minimize the probability of damage or destruction of the fire suppression system during the crash test. A redundant system configuration was selected to provide some fire suppression capability if one or more of the system components were damaged or destroyed in during the crash test. Spent or damaged components were replaced after the crash test.

The intent of the crash test was to determine the effectiveness of the fire suppression system under the scenario of a frontal crash resulting in a fire in the engine compartment of the test vehicle. In the crash test the fire suppression system was installed in the engine compartment of the test vehicle. The test vehicle was stationary and was struck in the left front by a moving barrier. The rational for selecting a 1999 Honda Accord and the frontal crash test protocols used in this test was as follows. A previous crash test of a 1998 Honda Accord using the same frontal crash test protocol as used in the crash test described in this report resulted in a fire in the engine compartment of the test vehicle [1]. The Honda Accord has the same body architecture for model years 1998 and 1999. No incendiary devices or other artificial means of causing a fire were used in this crash test; therefore, there was no certainty that a fire would occur during the crash test.

After the crash test, multiple fire tests were conducted using the crash-tested vehicle where the severity of the fire was increased until the limit of effectiveness of the suppression system was reached. These tests are referred to as static fire tests to denote the lack of vehicle motion and changes in the vehicle structure (i.e., dynamic crush). Both SPGG units were checked for proper weight and squib continuity and the operation of the optical flame detectors were checked before each static fire test. Static fire tests used a number of scenarios for ignition of a fire in the engine

compartment of the test vehicle. These scenarios included auto ignition of polymeric materials in contact with resistively heated electrical wiring and auto ignition of a combustible fluid on a heated surface.

Although the crash-tested vehicle was used for these static fire tests, these tests did not include a number of factors that may occur in an actual vehicle crash. These differences may lead to differences in the performance of an active fire suppression system. One example is vehicle motion. Vehicle motion during and after a crash may effect the distribution of fuel and other possible ignition sources in and around the vehicle. Vehicle motion creates airflow around and through the vehicle, which may affect both the pattern of distribution and concentration of fire suppression agent. As vehicle movement after a crash may involve both translation and rotation about one or more vehicle axis with changing accelerations, it is impossible to simulate airflow from this type of motion when the test vehicle is stationary. Another example is vehicle crush. The structural deformation that occurs during a crash can change the size and geometry of the engine compartment substantially, affecting how the fire suppression agent is distributed. As with vehicle movement, these changes in the vehicle's structure are complex and impossible to simulate in a static test. Another difference between a vehicle in a static fire test and a vehicle in an actual crash is component temperature. During the static fire tests where the engine was not running, all components in the test vehicle were at ambient temperature. Whereas, during an actual vehicle crash (and the crash tests conducted here), the engine is running and components in the engine compartment and the exhaust system are at temperatures greater than the ambient temperature. The elevated temperature may affect both the flammability properties of the materials used in motor vehicles and the effectiveness of the fire suppression agent. It is impractical to simulate road-load temperatures in a stationary test vehicle, especially when the engine has been damaged in a crash test and is inoperable.

The criteria for assessing the effectiveness of the suppression systems were (i) the ability of the fire suppression systems tested in this study to remain functional after the crash test, (ii) the ability of the fire suppression systems tested in this study to extinguish fires, if any, that occurred during or after the crash tests, and (iii) the ability of the systems tested in this study to extinguish fires during the static tests.

3.1 Frontal Crash Test

This crash test resulted in a fire in the engine compartment of the test vehicle. A review of high-speed film of this crash test showed flames in the area of the exhaust manifold starting at about 184 ms after time zero. Figure 5 is a frame grab from the high-speed film in the camera mounted

Figure 5. Crash Test C12610. High-speed film frame grab from the camera mounted on the right front fender of the test vehicle at 220 ms after time zero. The hood deformed upward and the engine compartment is visible under the right edge of the hood.

on the right front fender after time zero showing flames in the area between the front of the engine and the upper radiator cross member at 220 ms after time zero. The gas chromatography / mass spectrometry data in Appendix C shows the presence of power steering fluid vapor / aerosol in the space between the exhaust manifold and the exhaust manifold heat shield. The temperature data in Appendix D indicates that the temperature of the exhaust manifold runner was sufficient to result in autoignition of power steering fluid in contact with this section of the exhaust manifold [9].

Data recorded from the fire suppression system indicates that Detector 1 output a firing signal at 298 milliseconds. Detector 2 did not output a firing signal at any time during this test. The system was configured so that an alarm from either of the two detectors caused the two gas generator extinguishers to discharge (see Appendix E). Thus, the firing signal from Detector 1 caused both SPGG units to discharge.

The fact that, initially, only detector 1 alarmed, is consistent with the physical location of the fire which ignited on the left side of the engine compartment. It is therefore reasonable that Detector 2 did not alarm initially. Detector 2 may not have alarmed to the subsequent re-flash[3] fire due to crash effects including: a) damage to this detector sustained in the crash and b) re-orientation of the detector so that the sensing element did not "see" radiation from the flames.

The fire suppression system failed to extinguish the fire. The result was that the fire was, at most, briefly knocked down. The fire in the engine compartment continued to burn after the suppression system discharged. The fire was extinguished manually using a deluge gun on a pumper truck present for this test.

Figure 6 shows a series of high-speed film frame grabs at 280, 360, 1200, and 2700 ms after time zero. Close inspection of the frame grab at 280 ms after time zero shows flames visible in the front of the engine compartment in the approximate location of the exhaust manifold (Fig. 6). The frame grab at 380 and 1200 ms after time zero show the effluent from the SPPG units venting

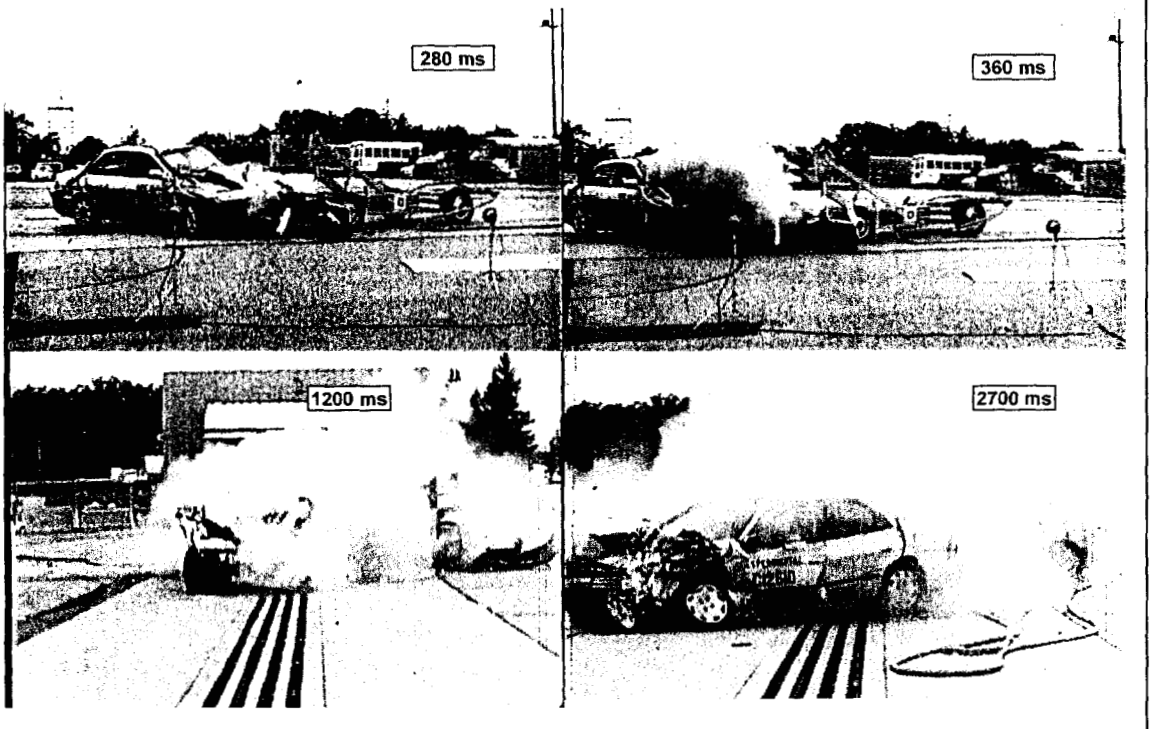

Figure 6. Crash Test C12610. High-speed film frame grabs at 280, 360, 1200, and 2700 ms after time zero.

[3] Re-flash is defined as re-ignition of gasoline vapor after the fire was initially extinguished by the SPGG fire suppression system. The fire suppression system did not eliminate potential ignition sources on the test vehicle and therefore did not result in permanent extinguishment.

from the engine compartment through gaps between the deformed hood and the front fenders during this crash event (Fig. 6). The frame grab at 2700 ms after time zero shows flames emerging from under the front of the engine compartment after the test vehicle and fire suppression agent had dispersed out of the engine compartment (Fig. 6).

The failure of the automatic extinguishers to significantly suppress or extinguish the fire was probably due to the effects of vehicle deformation and motion during the crash test, which re-directed and altered the discharge pattern of suppression agent from the SPGG units. The hood remained latched and the center of the hood deformed upward as the barrier crushed the front of the test vehicle, creating gaps between the sides of the hood and the front fenders and between the rear of the hood and the cowl. Vehicle rotation combined with wind (3 to 5 mph steady with 8 to 10 mph gusts out of the West) effectively cleared the suppression agent from the engine compartment through these gaps before the vehicle came to rest. This lead to a reduction in the amount of suppression agent distributed to the flames because a large fraction of the effluent from the SPGG units was not contained within the engine compartment and dispersed outside of the engine compartment, without attacking the fire.

Another factor contributing to the failure of the fire suppression system to extinguish the fire in this test appears to be ineffective distribution of agent into the lower portion of the engine compartment because of crush to the front of the test vehicle. The optical detectors and SPGG units were located on the hood to minimize the possibility of physical damage to the fire suppression system during the crash test. Previous testing indicated that fire detectors located on the hood of a vehicle involved in a frontal crash test were less likely to fail because of direct impact or crushing damage than fire detectors located elsewhere in the engine compartment [1, 10 - 12]. With the SPGG units located on the hood, effective flame suppression requires distribution of the agent downward into the engine compartment. Inspection of the test vehicle after this crash test indicated that crush of the front of the test vehicle reduced the volume of airspaces between objects and created restricted voids in the engine compartment that were not present in the un-crashed vehicle. Lack of containment within the engine compartment caused by rapid dispersion of agent out of the engine compartment during this crash test appears to have resulted in distribution of insufficient amounts of agent for fire suppression into the air spaces in the lower part of the engine compartment, as evidenced by observations of flames in the lower engine compartment while the test vehicle was rebounding from the barrier and after it came to rest (Fig. 6).

3.2 Static Fire Tests

A series of four static fire tests were conducted using the vehicle that had been subjected to the crash test. For the static fire tests, the vehicle was stationary, and the engine and other components in the engine compartment were at ambient temperature. Spent or damaged components of the suppression system were replaced after each static fire test. Two new, fully charged, SPGG units were installed in the test vehicle before each test. Except for the first test, fires in the engine compartment were ignited using an electrical igniter or by spraying a combustible oil onto a surface heated by electrical heaters. In both cases, electrical power was supplied to the igniters by gasoline-powered generator. The optical flame sensor was tested before each test to determine if it functioned within specifications. The test involved exposing each sensor to a test flame and monitoring its output signal. The optical flame sensor was determined to be functioning within specifications prior to each of the four static fire tests.

3.2.1 Static Test F990812A - Manual SPGG Discharge without Fire in the Engine Compartment

This test was conducted to determine the effect of the fire suppression system on under-hood components. No fire was started in the test vehicle for this test. The fire suppression system was activated by a remote manual trigger. The hood liner, HVAC air intake cowl, and power distribution box cover had all been damaged during the crash test and were replaced before this first static fire test. Electrical power for the system was supplied by an external battery. Power steering fluid and engine coolant (1:1 ethylene glycol-water) were sprayed into the engine compartment as the units were triggered. The discharge from the SPGG units (Fig. 7) blew sections of the hood liner out of the engine compartment onto the ground around the test vehicle.

After activation of the SPGG units, fragments of the hood liner were found in the engine compartment of the test vehicle and on the ground around the front of the test vehicle. The heated gas discharge from the SPGG units appeared to ignite combustible materials in the hood liner.[4] Smoke was observed rising from the hood liner fragments in the engine compartment and on the ground. Glowing embers were observed in some of the fragments of hood liner where the binder in the hood liner was not burned-off completely during the initial SPGG discharge.

[4] The hood liner in the test vehicle consisted of a glass fiber mat with a phenolic binder. The combustible material in the hood liner was the phenolic binder.

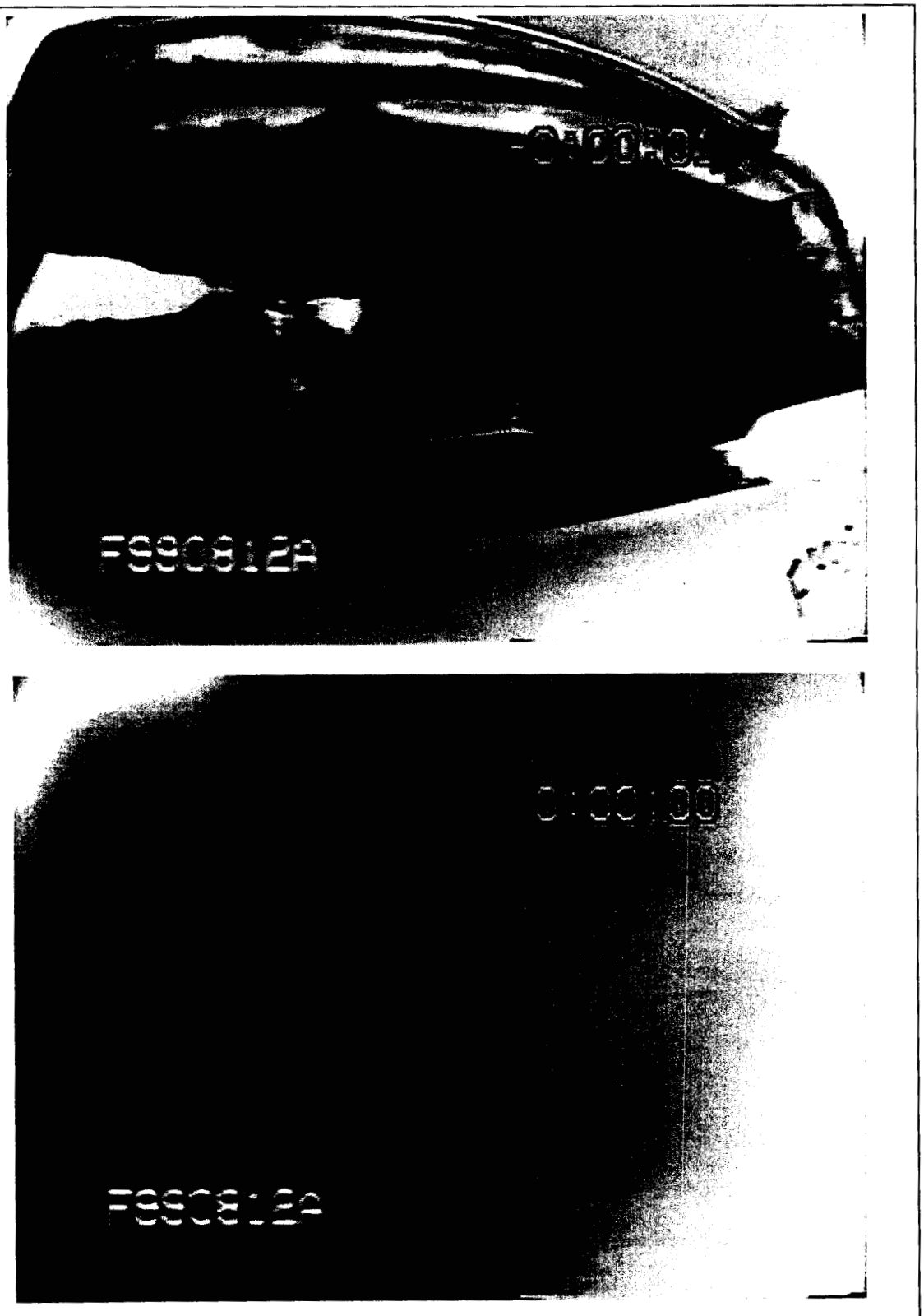

Figure 7. Static Test F990812A. View from hood just prior to manual SPGG discharge (upper) and during discharge (lower).

3.2.2 Static Fire Test F990812B – Electrical Ignition of Plastic

An electrical igniter was placed under the cover of the power distribution box. The damaged hood liner was removed and a new hood liner was installed in the test vehicle. The spent SPGG units were removed and two charged SPGG units installed on the hood of the test vehicle. One of the optical flame detectors was not functioning within specifications, and was removed from the circuit. To start the test, electrical current was applied to the igniter, which resulted in flaming ignition of plastic materials in the power distribution box in approximately 90 seconds. The optical flame detector triggered discharge of the SPGG units shortly after flames were first visible. The discharge from the fire suppression system initially extinguished the flames. The igniter remained energized and a fire re-ignited in the area of the igniter within a few seconds (approximately 18 seconds after ignition). The sequence is shown in Figure 8. Safety personnel present for this test extinguished the fire using hand-held fire extinguishers (carbon dioxide).

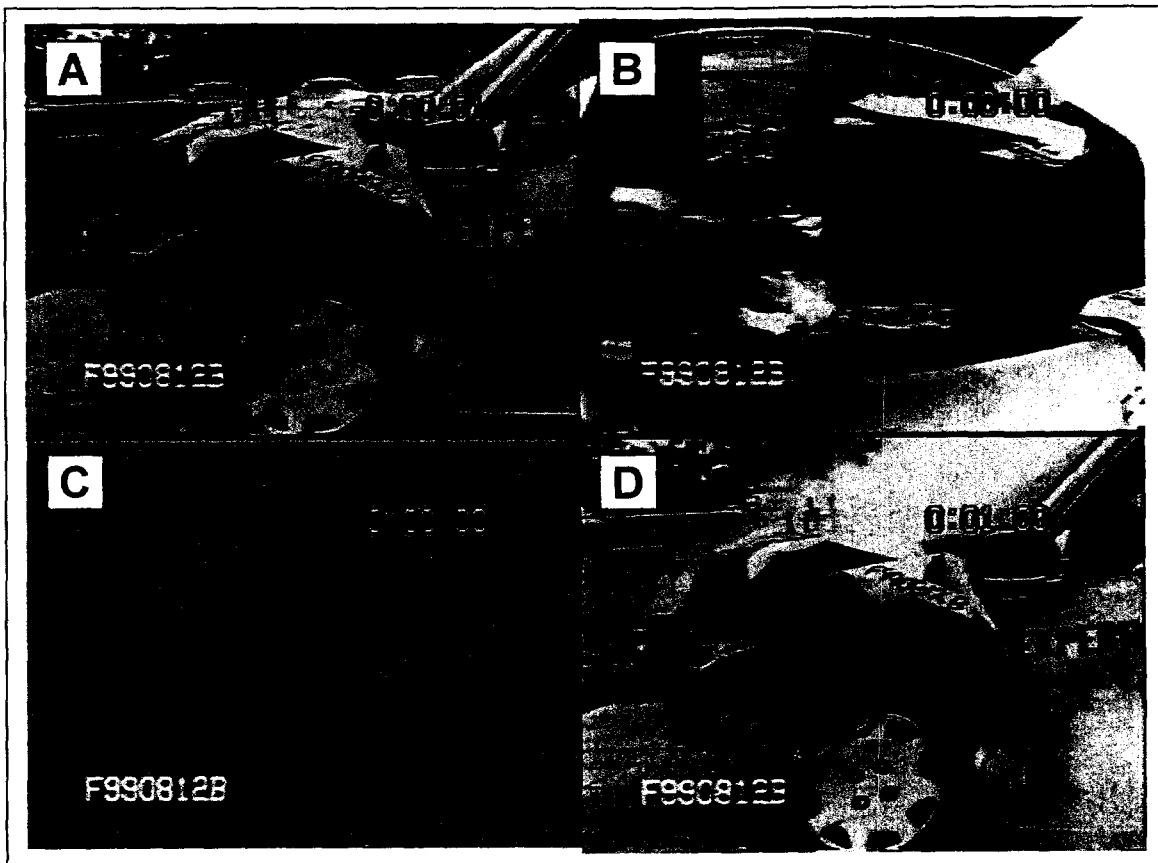

Figure 8. Static Fire Test F990812B. Video stills showing side view 1 second discharge (A), flame apparent in the engine compartment view just prior to detection (B), discharge of the SPGG units (C), and re-flash fire apparent at 1 min after discharge of the SPGG units (D).

3.2.3 Static Fire Test F990812C – Autoignition of Power Steering Fluid

A heated metal plate was placed on top of the exhaust manifold heat shield and a fine mist of power steering fluid was sprayed onto the plate. The spent SPGG units were removed and two charged SPGG units installed on the hood of the test vehicle. Although the hood liner was damaged in the previous test, it was left in place on the hood because no more undamaged hood liners were available. To start the test, electrical power was supplied to the electrical heaters in the metal plate. When the temperature of the metal plate exceeded 400°C, the power to the electrical heaters was shut-off and the power steering fluid was sprayed onto the upper surface of the plate. Three attempts were required to achieve autoignition of the power steering fluid on the heated metal plate. The deformed hood allowed wind into the engine compartment of the test vehicle during this test.[5] Airflow over the heated plate appeared to have prevented autoignition of the power steering fluid by (i) diluting the power steering vapor so that the vapor concentration was less than the lower flammability limit, and (ii) cooling the vapor / air mixture so that the gas temperature was less than the autoignition temperature of power steering fluid in air.[6]

Autoignition of the power steering fluid on the heated metal plat was finally achieved by placing a barrier along one side of the metal plant to shield it from wind blowing through the engine compartment. The optical flame detector triggered discharge of the SPGG units shortly after flames were first observed in the engine compartment. The flames were extinguished, but re-ignition of residual power steering fluid on the metal plate occurred shortly after the discharge from the units had ceased, approximately 37 seconds after the first fire was detected. The sequence is shown in Figure 9. Safety personnel present for this test extinguished the fire using hand-held fire extinguishers (carbon dioxide).

---

[5] The wind speed at the test vehicle at the time of this test was measured with hand-held anemometer. The wind speed was estimated to be 5 – 10 mph. The direction of the wind was from right to left relative to the test vehicle.

[6] Power steering fluid used in motor vehicle is typically a petroleum-based hydrolic fluid. The lower flammability limit of power steering fluid is approximately 1% (ASTM E681-98). The autoigintion temperature of power steering fluid is in the range of 350 - 400°C (ASTM E659-78).

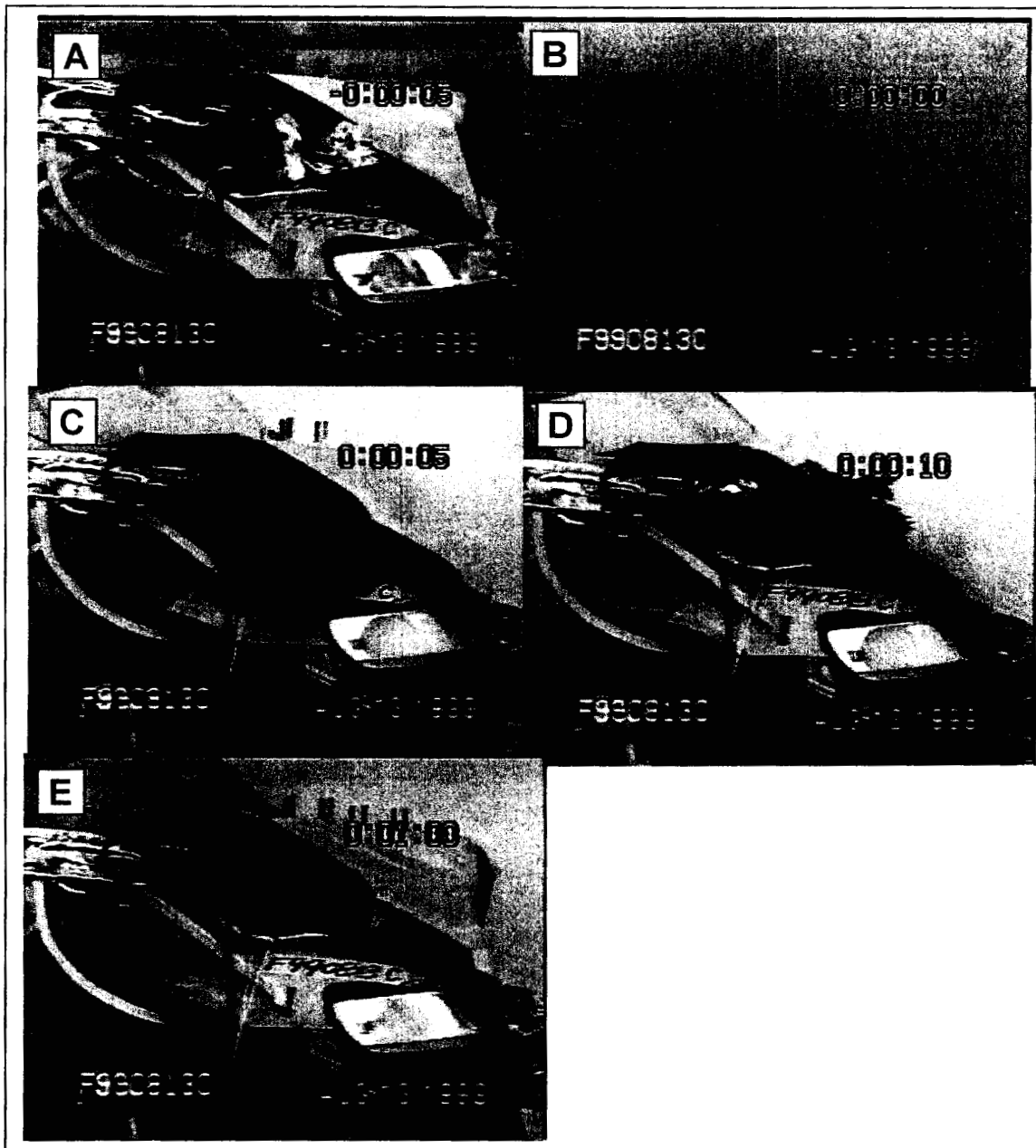

Figure 9. Static Fire Test F990813C. Video stills showing flames in engine compartment 5 seconds before SPGG discharge (A), automatic discharge of the SGG units (B), knock-down of the flame at 5 seconds after discharge (C), a re-flash fire on the hood liner 10 sec after discharge of the SPGG units (D), and flames from re-ignition of residual power steering fluid on the heated plat 1 minute after discharge of the SPGG units (E).

3.2.4 Static Fire Test F990812D – Electrical Ignition of Plastic

An electrical igniter was placed on top of the battery. The spent SPGG units were removed and two charged SPGG units installed on the hood of the test vehicle. To start the test, electrical current was applied to the igniter. Flaming ignition of the plastic materials in the igniter was observed in approximately 90 sec. Electrical power to the igniter was shut-off as soon as flaming ignition was observed. Although the optical fire detector functioned properly before and after this test, the optical fire detector failed to activate the fire suppression system. The SPGG units were activated using a remote manual trigger connected to an external power supply. The flames were extinguished by the discharge from the SPGG units. Re-ignition did not occur. The optical flame sensor was tested after this test and determined to be functioning within specifications. Figure 10 shows the flame and SPGG discharge.

Figure 10. Static Fire Test F990813D. Video stills showing flames under hood 15 sec before discharge of the SPGG units (A), flames in the engine compartment 2 seconds before discharge of the SPGG units (B), manual discharge of the SPGG units (C), and complete extinguishment of flames in the engine compartment 10 sec after discharge of the SPGG units (D).

4 Summary and Conclusion

Prototype fire suppression systems installed in a test vehicle did not extinguish fires in the crash test and in two of the three static vehicle fire tests described in this report. The fire that occurred in the crash test was detected but not extinguished. A test of the gas generator suppression system did not in itself cause a fire, but evidence of ignition of combustible materials in the hood liner by heated gases in the SPGG discharge was observed after the test. Of the three post-crash static fire tests performed, the optical fire detector sensed fire and triggered the SPGG units in two of these tests. In both of these tests, flames were suppressed temporarily for 18 and 37 seconds before a second, re-flash fire appeared. In the post-crash static fire test where the detector failed to alarm, the SPGG units were triggered manually, suppressing flames without a re-flash. Thus, the SPPG fire suppression system tested here did not extinguish flames in the engine compartment of a test vehicle in one crash test and in two of three static vehicle fire tests.

The results of the crash and fire tests described in this report differ markedly from results of testing reported by NIST [2], which suggested that fire suppression systems based on optical detectors and solid propellant gas generators may be effective in suppressing fires in the engine compartments of passenger vehicles. The tests conducted by NIST involved evaluation of fire suppression systems based on Halon Replacement gaseous agents, dry powder agents, and Solid Propellant Gas Generators. These systems were tested in laboratory tests using engine compartment mock-ups or in the engine compartment of a stationary vehicle with no crash damage. These tests did not simulate real-world dynamic events such as vehicle motion, vehicle crush, or airflow through the engine compartment that occur during a vehicle crash and affect the concentration and distribution of agent within the engine compartment. These dynamic factors appear to explain the differences between the results of the tests conducted by NIST [2] and the tests described in this report.

References

1. Jack L. Jensen and Jeffrey Santrock. Evaluation of Motor Vehicle Fire Initiation and Propagation. Part 11: Crash Tests on a Front-Wheel Drive Passenger Vehicle. Submitted to the National Highway Transportation Safety Administration pursuant to the Settlement Agreement between General Motors and the Department of Transportation. Submitted May 7, 2002.

2. Anthony Hammins. Evaluation of Active Suppression in Simulated Post-Collision Vehicle Fires. Submitted to the National Highway Transportation Safety Administration pursuant to the Settlement Agreement between General Motors and the Department of Transportation. Submitted March 7, 2001.

3. Hodges, S.E. and Simpson, G. D., "Effective Technologies for Fire Sensing and Suppression on Transit Vehicles," American Public Transportation Association (APTA), Bus Operations and Technologies Conference, May 1995

4. Chattaway, A. C., et al, "The Evaluation of Non-Pyrotechnically Generated Aerosols as Fire Suppressants," Halon Options Technical Working Group (HOTWC), Albuquerque, April 1995.

5. Fire Protection Handbook, "Quantity and Rate of Application of Dry Chemical," p. 6-346, 18th Edition, National fire Protection Association, Quincy, MA, 1997.

6. Vehicle and Mobile Machinery Fire-Extinguishing Systems, Instruction Manual, Kidde Fire Systems, P/N 83-131005-001, Feb. 2001.

7. Yang, J. C. and W. L. Grosshandler, editors, "SOLID PROPELLANT GAS GENERATORS: PROCEEDINGS OF THE 1995 WORKSHOP," NISTIR 5766, NIST, Gaithersburg, MD, Nov. 1995.

8. An explanation of the Joule-Kelvin effect can be found in most Physical Chemistry texts.

9. Jeffrey Santrock and Douglas W. Kononen. Project B.10 – Study of Flammability of Materials. Flammability Properties of Engine Compartment Fluids Other than Gasoline. AutoIgnition Characteristics of Non-Gasoline Motor Vehicle Fluids on Heated Surfaces. Submitted to the National Highway Transportation Safety Administration pursuant to the Settlement Agreement between General Motors and the Department of Transportation. Submitted September 30, 2002.

10. Jack L. Jensen and Jeffrey Santrock. Evaluation of Motor Vehicle Fire Initiation and Propagation. Part 2: Crash Tests on a Passenger Van. Submitted to the National Highway Transportation Safety Administration pursuant to the Settlement Agreement between General Motors and the Department of Transportation. Submitted September 1, 1998.

11. Jack L. Jensen and Jeffrey Santrock. Evaluation of Motor Vehicle Fire Initiation and Propagation. Part 5: Crash Tests on a Rear Wheel Drive Passenger Car. To be submitted to the National Highway Transportation Safety Administration pursuant to the Settlement Agreement between General Motors and the Department of Transportation.

12. Jack L. Jensen and Jeffrey Santrock. Evaluation of Motor Vehicle Fire Initiation and Propagation. Part 8: Crash Tests on a Sport-Utility-Vehicle. Submitted to the National Highway Transportation Safety Administration pursuant to the Settlement Agreement between General Motors and the Department of Transportation. February 15, 2001

Appendix A

Accelerometer Data

Crash Test C12610

Five tri-axial (longitudinal, lateral, and vertical) accelerometers were mounted to each of the test vehicles in the following locations:

- Right front rocker panel
- Left front rocker panel
- Right Rear Rocker Panel
- Left Rear Rocker Panel
- Hood center

Figure A1 shows the approximate locations of the accelerometers on the test vehicle.

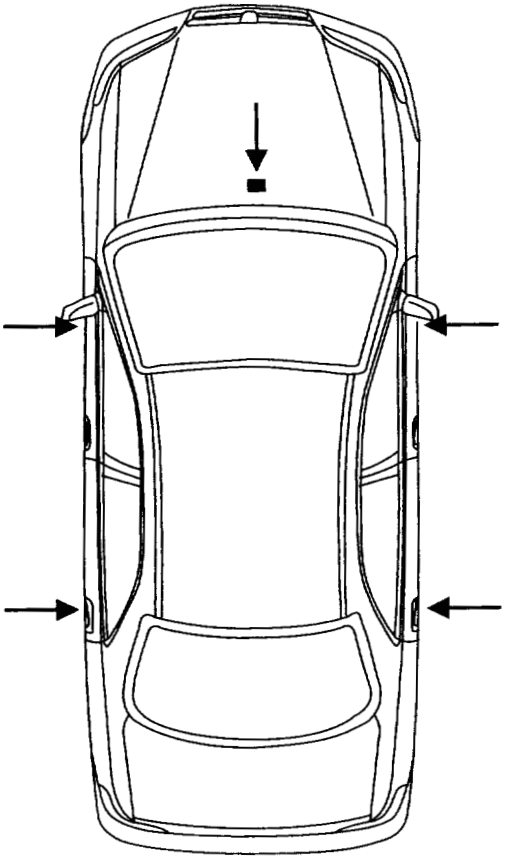

Figure A1. Diagram showing the approximate locations of the accelerometers on the test vehicle.

Two tri-axial (longitudinal, lateral, and vertical) accelerometers were mounted on the Adjustable Moving Deformable Barrier (AMDB) in the following locations:

- Rear cross member
- Center of Mass

Figure B1 shows the approximate locations of the accelerometers on the Adjustable Moving Deformable Barrier.

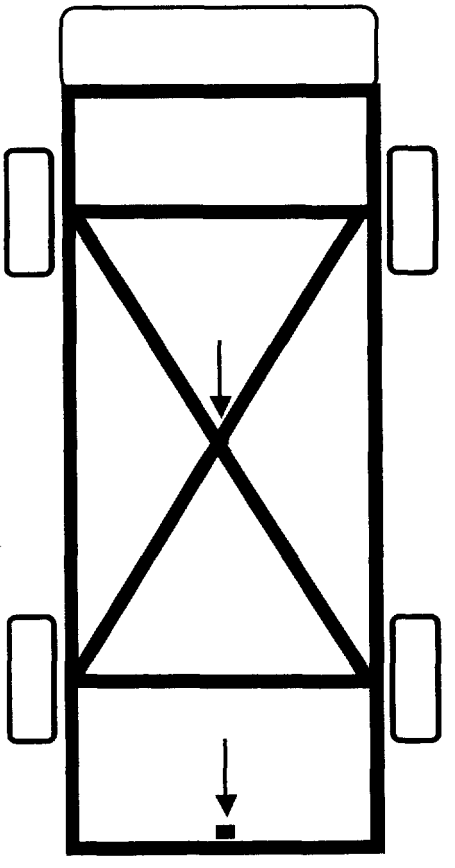

Figure A2. Diagram showing the approximate locations of the accelerometers on Adjustable Moving Deformable Barrier.

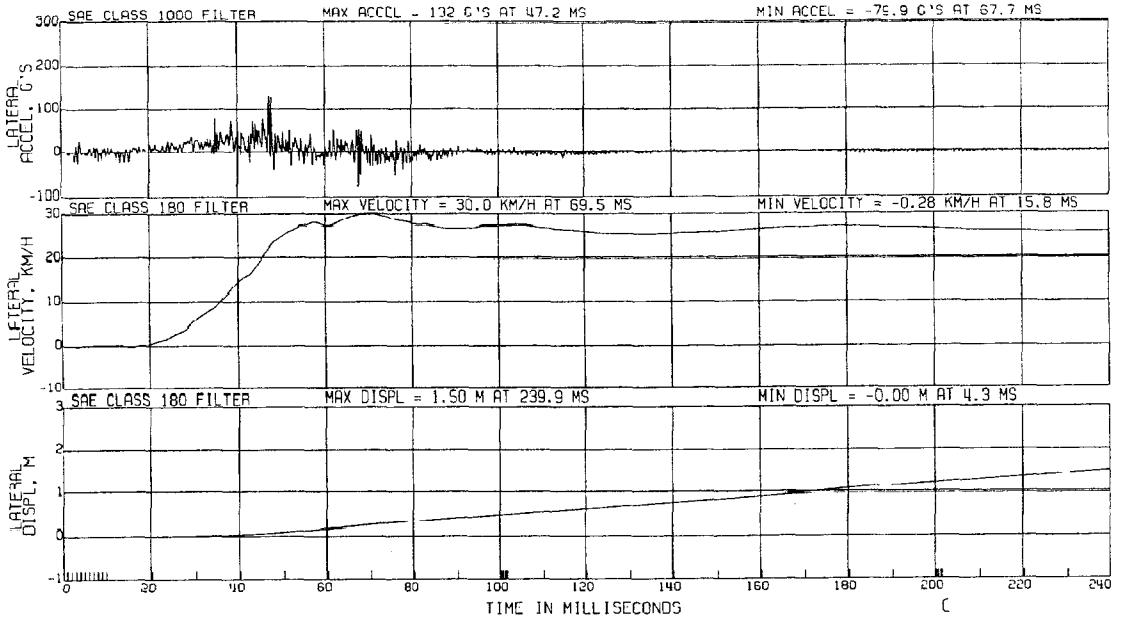

Plot A1. Crash Test C12610. Plots of acceleration, velocity, and displacement in the direction of the lateral-axis calculated from the accelerometer on the left front rocker.

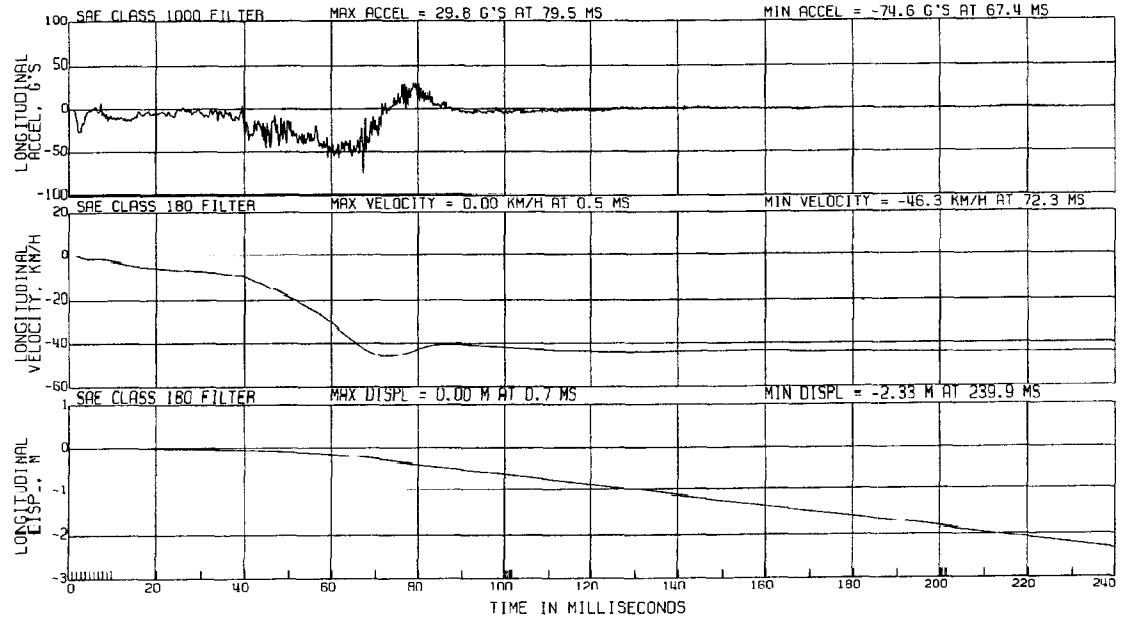

Plot A2. Crash Test C12610. Plots of acceleration, velocity, and displacement in the direction of the longitudinal-axis calculated from the accelerometer on the left front rocker.

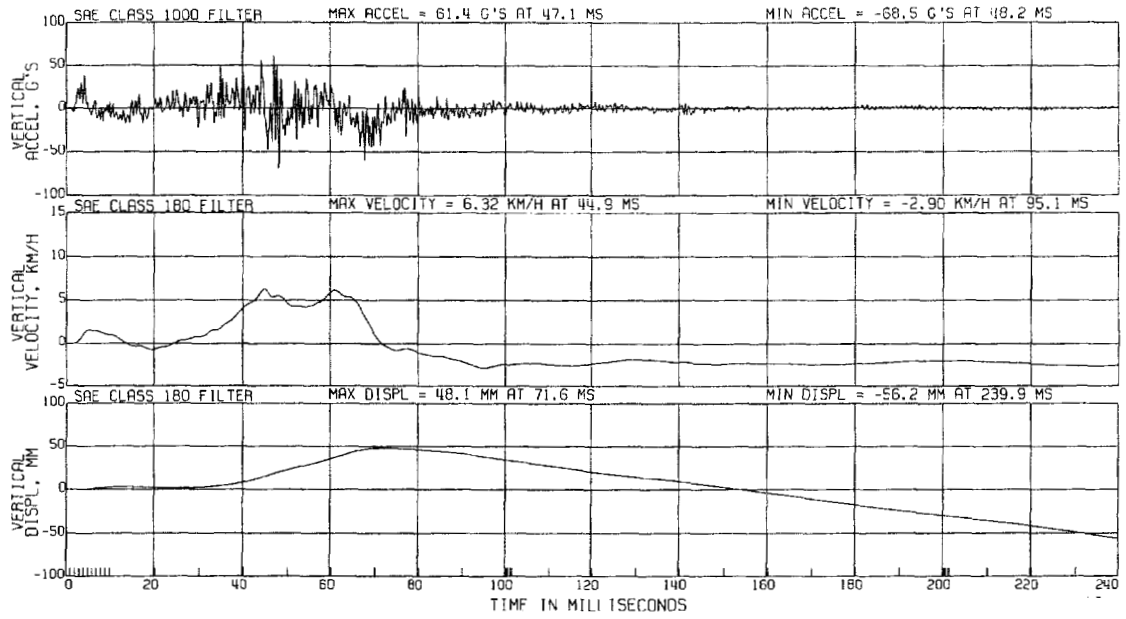

Plot A3. Crash Test C12610. Plots of acceleration, velocity, and displacement in the direction of the vertical-axis calculated from the accelerometer on the left front rocker.

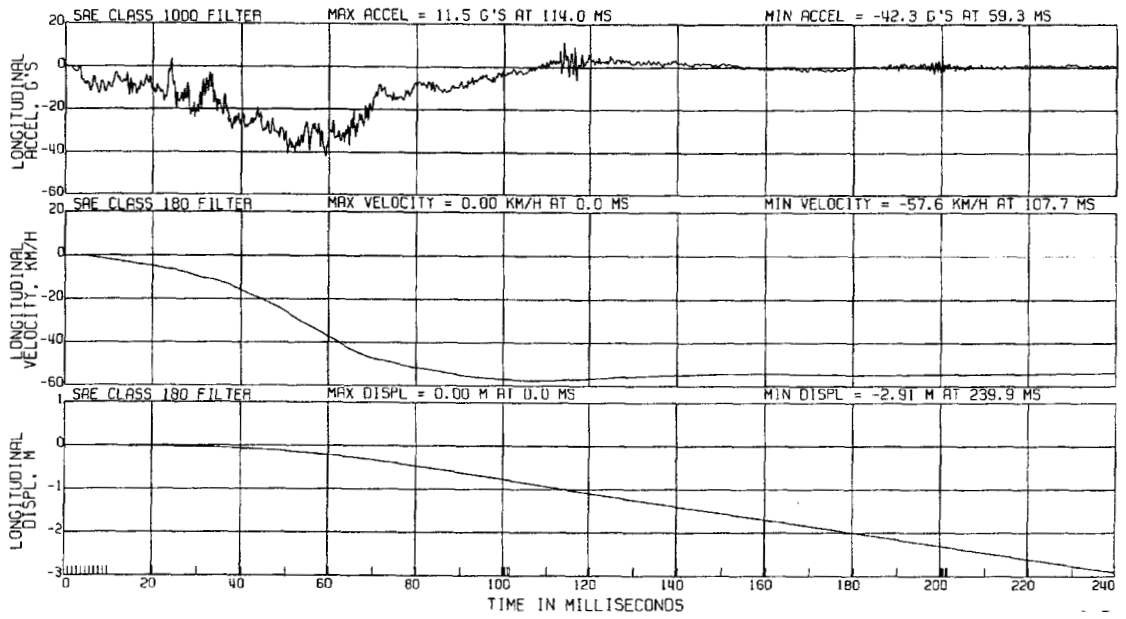

Plot A4. Crash Test C12610. Plots of acceleration, velocity, and displacement in the direction of the longitudinal-axis calculated from the accelerometer on the right front rocker.

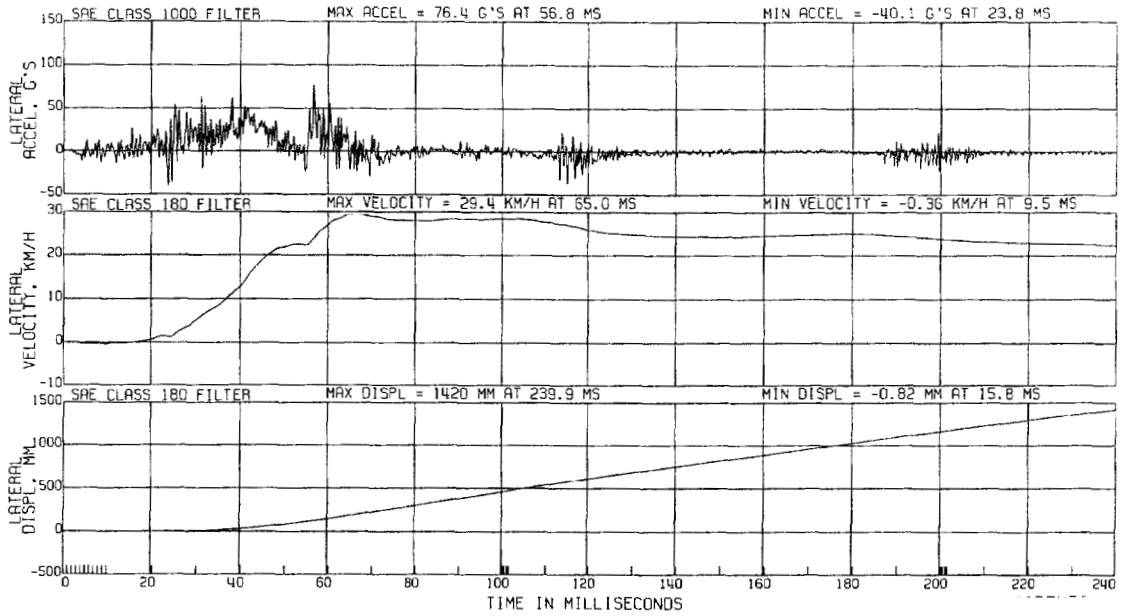

Plot A5. Crash Test C12610. Plots of acceleration, velocity, and displacement in the direction of the lateral-axis calculated from the accelerometer on the right front rocker.

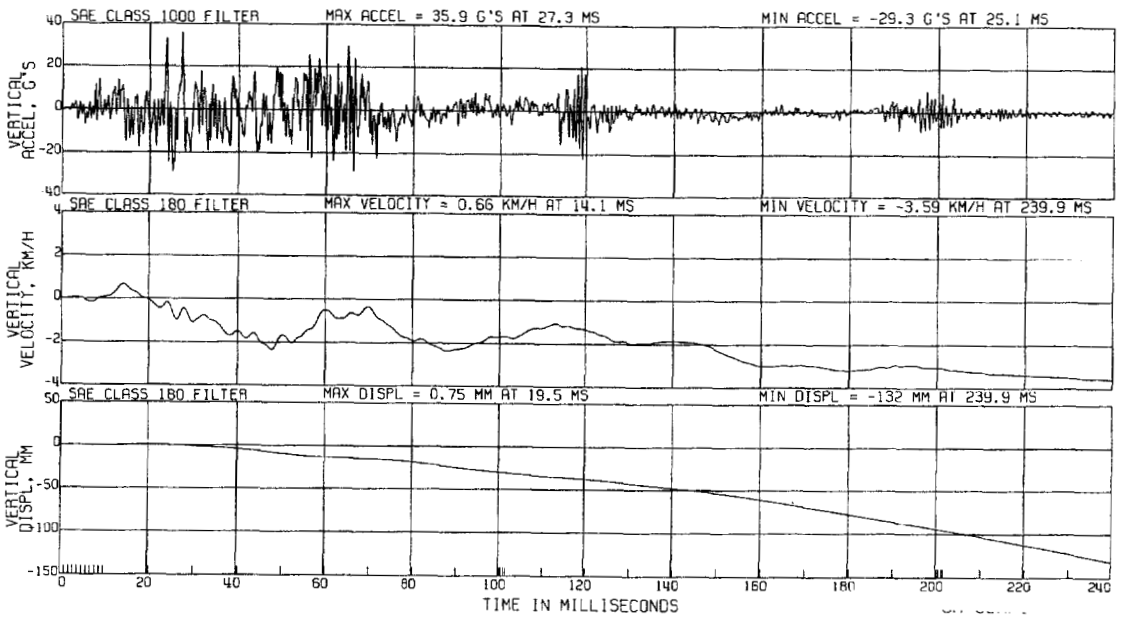

Plot A6. Crash Test C12610. Plots of acceleration, velocity, and displacement in the direction of the vertical-axis calculated from the accelerometer on the right front rocker.

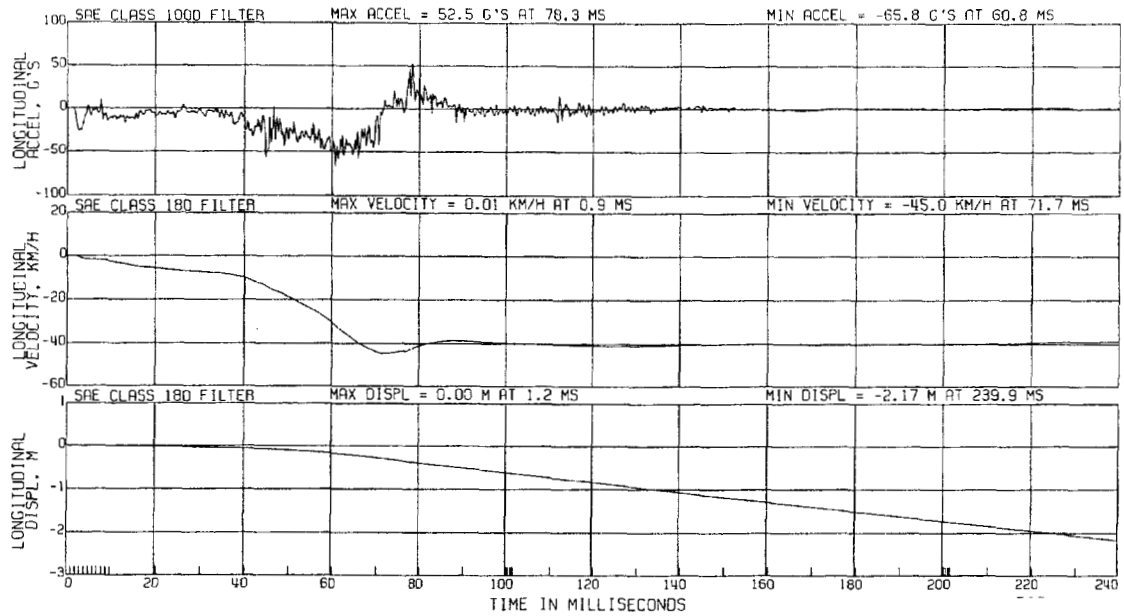

Plot A7. Crash Test C12610. Plots of acceleration, velocity, and displacement in the direction of the longitudinal-axis calculated from the accelerometer on the left rear rocker.

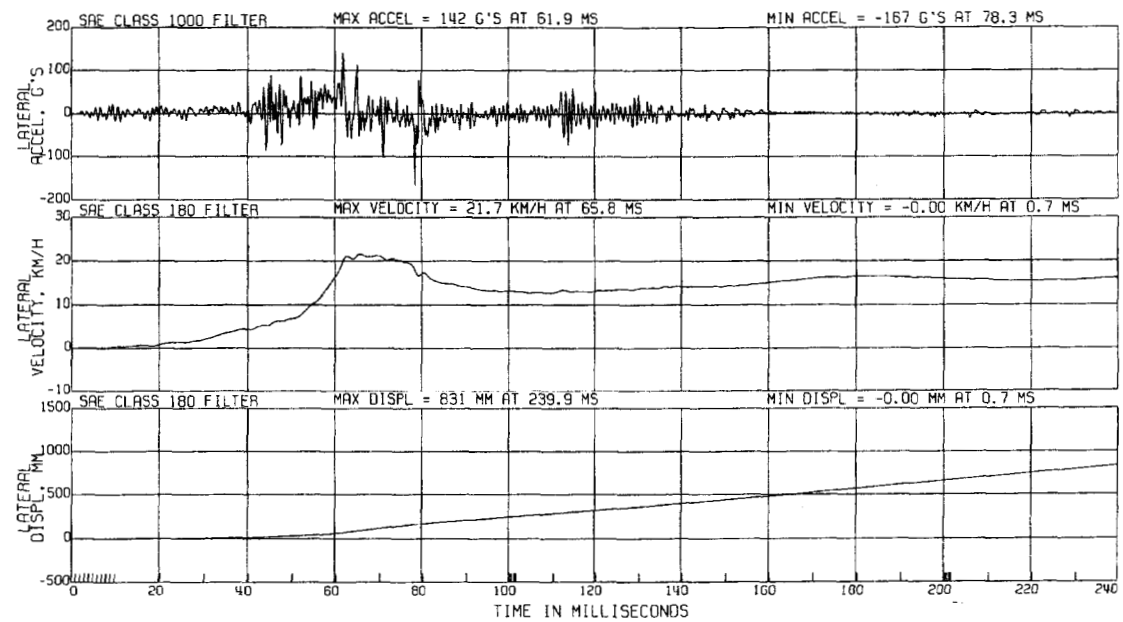

Plot A8. Crash Test C12610. Plots of acceleration, velocity, and displacement in the direction of the lateral-axis calculated from the accelerometer on the left rear rocker.

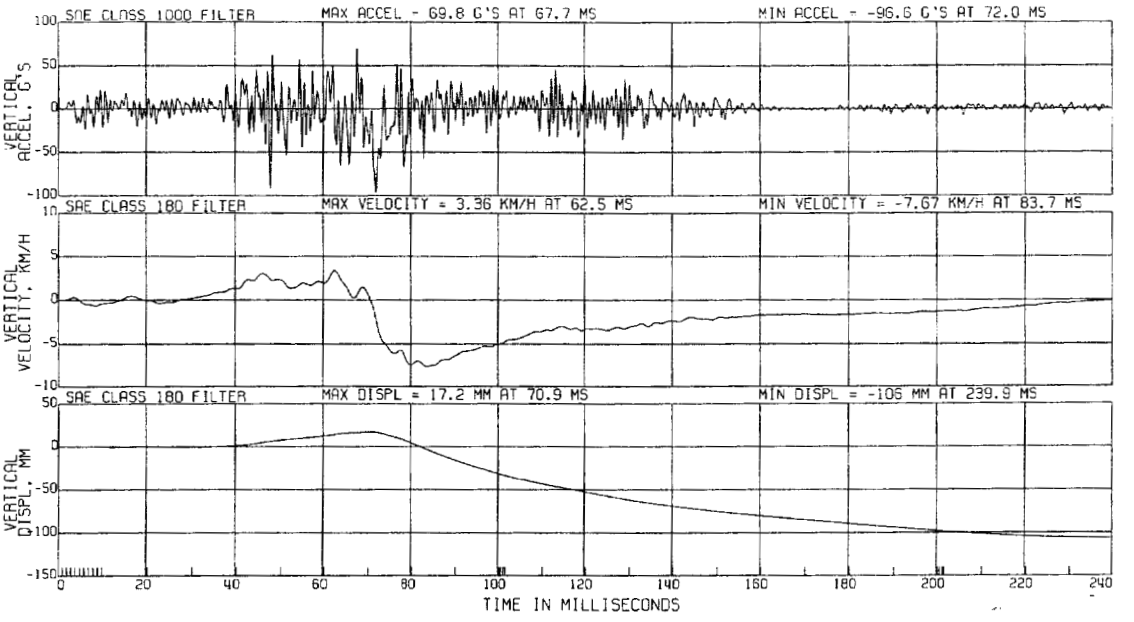

Plot A9. Crash Test C12610. Plots of acceleration, velocity, and displacement in the direction of the vertical-axis calculated from the accelerometer on the left rear rocker.

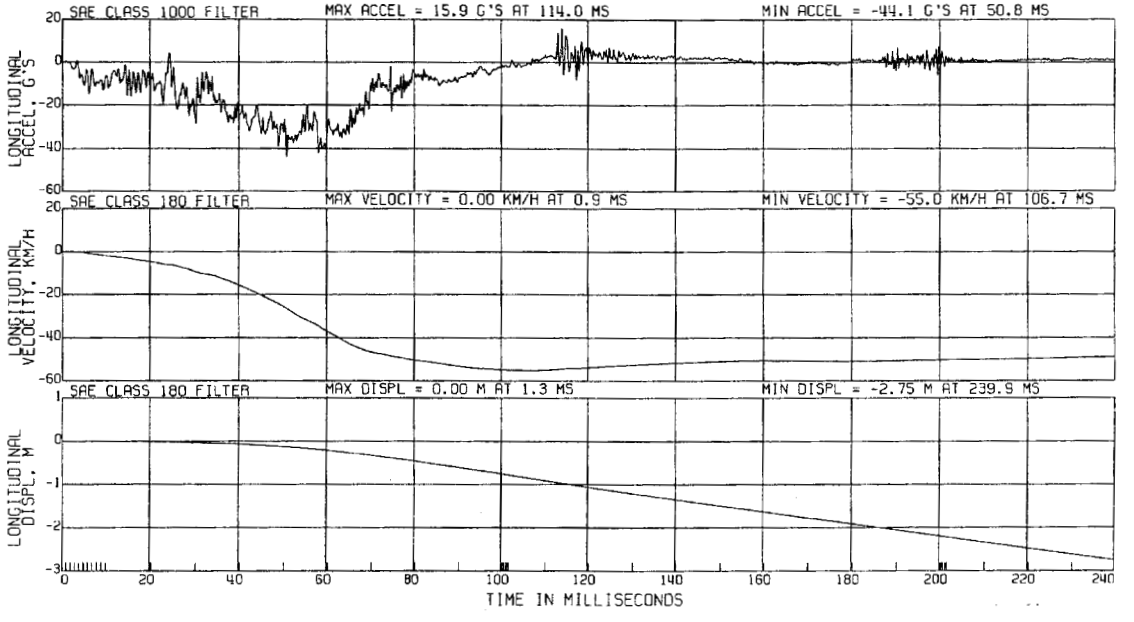

Plot A10. Crash Test C12610. Plots of acceleration, velocity, and displacement in the direction of the longitudinal-axis calculated from the accelerometer on the right rear rocker.

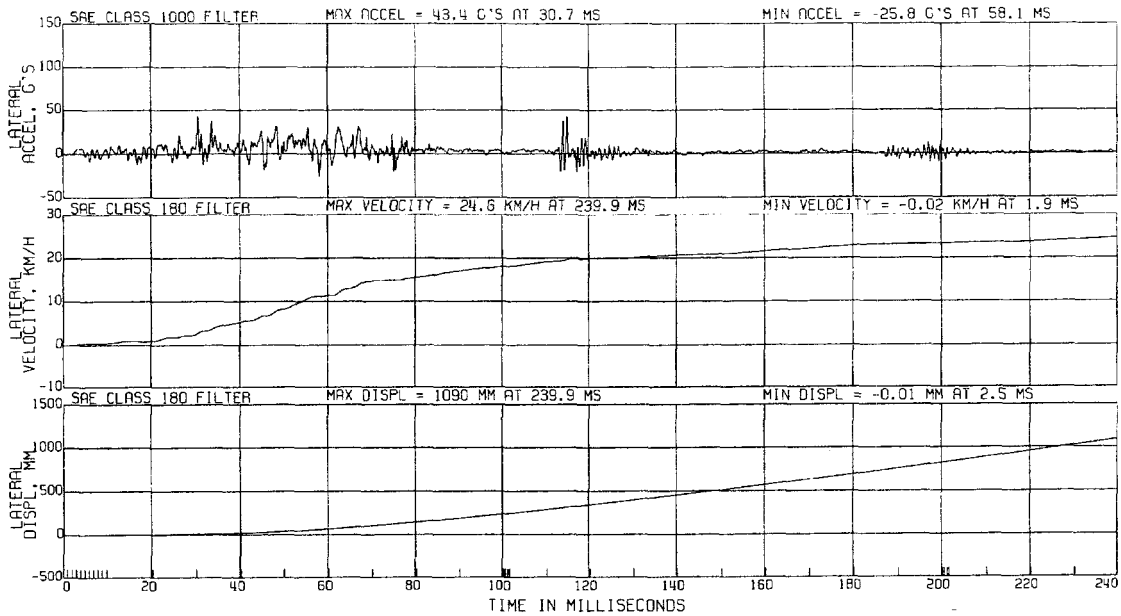

Plot A11. Crash Test C12610. Plots of acceleration, velocity, and displacement in the direction of the lateral-axis calculated from the accelerometer on the right rear rocker.

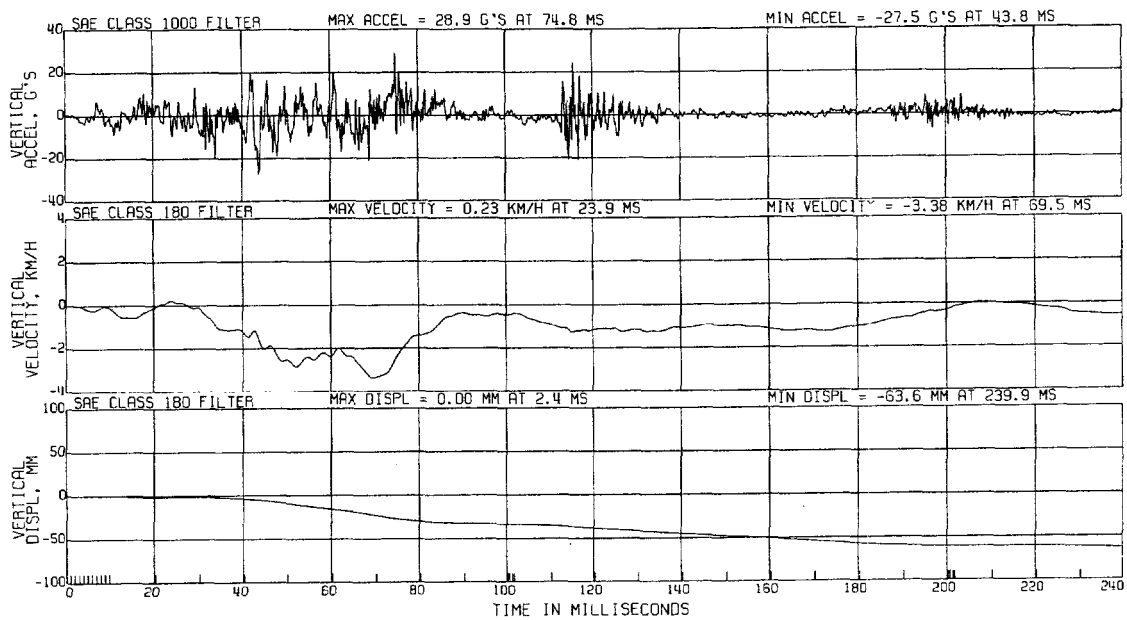

Plot A12. Crash Test C12610. Plots of acceleration, velocity, and displacement in the direction of the vertical-axis calculated from the accelerometer on the right rear rocker.

Appendicies

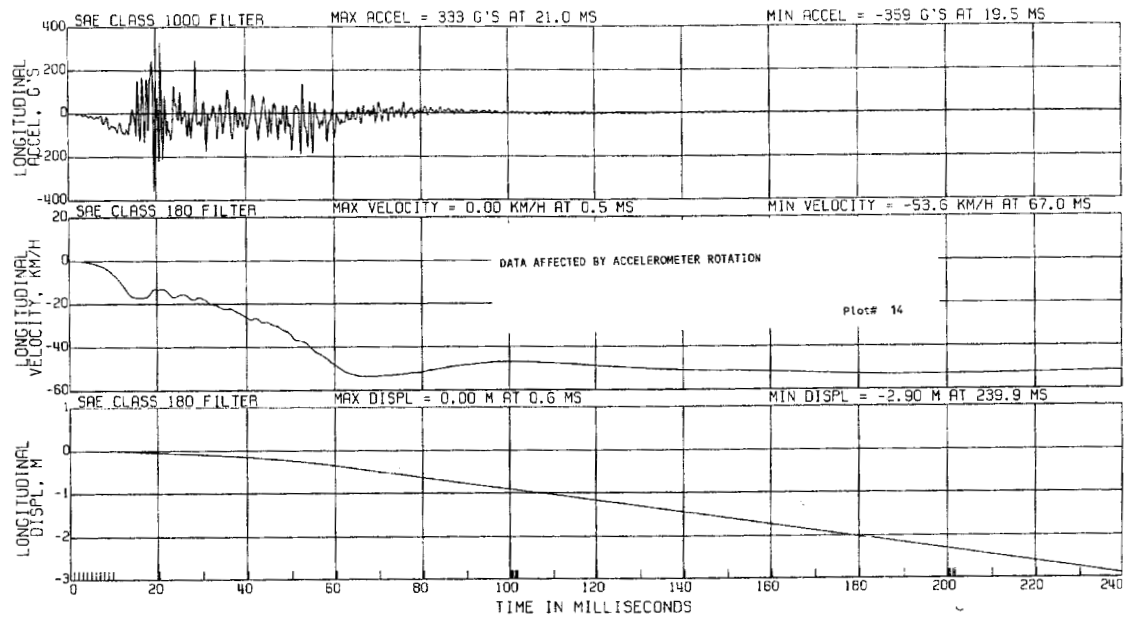

Plot A13. Crash Test C12610. Plots of acceleration, velocity, and displacement in the direction of the longitudinal-axis calculated from the accelerometer on the hood.

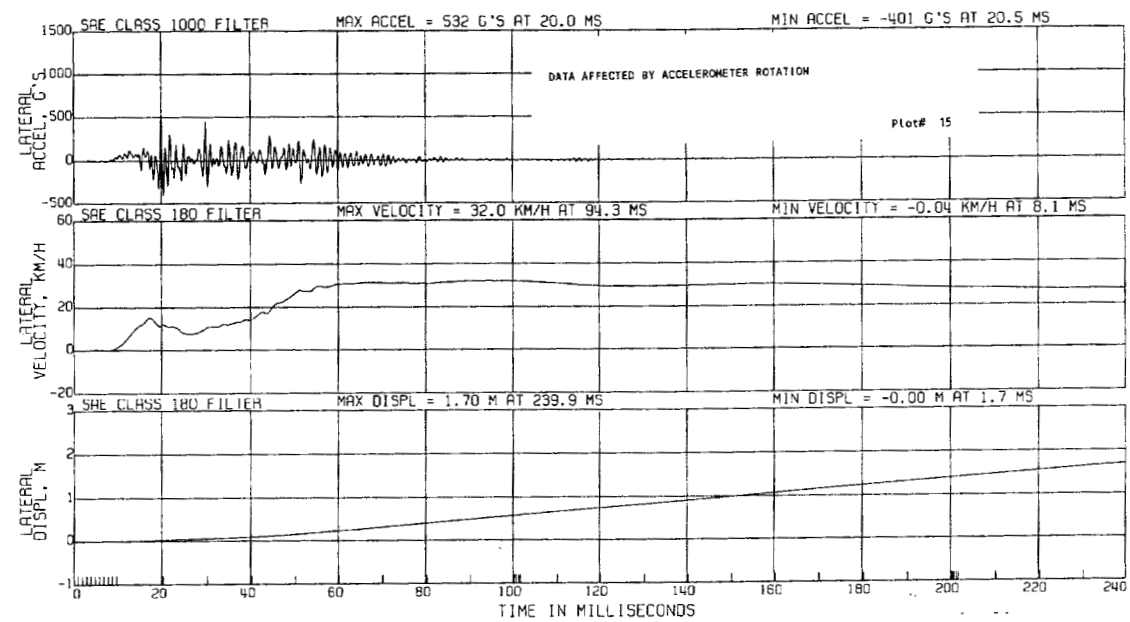

Plot A14. Crash Test C12610. Plots of acceleration, velocity, and displacement in the direction of the lateral-axis calculated from the accelerometer on the hood.

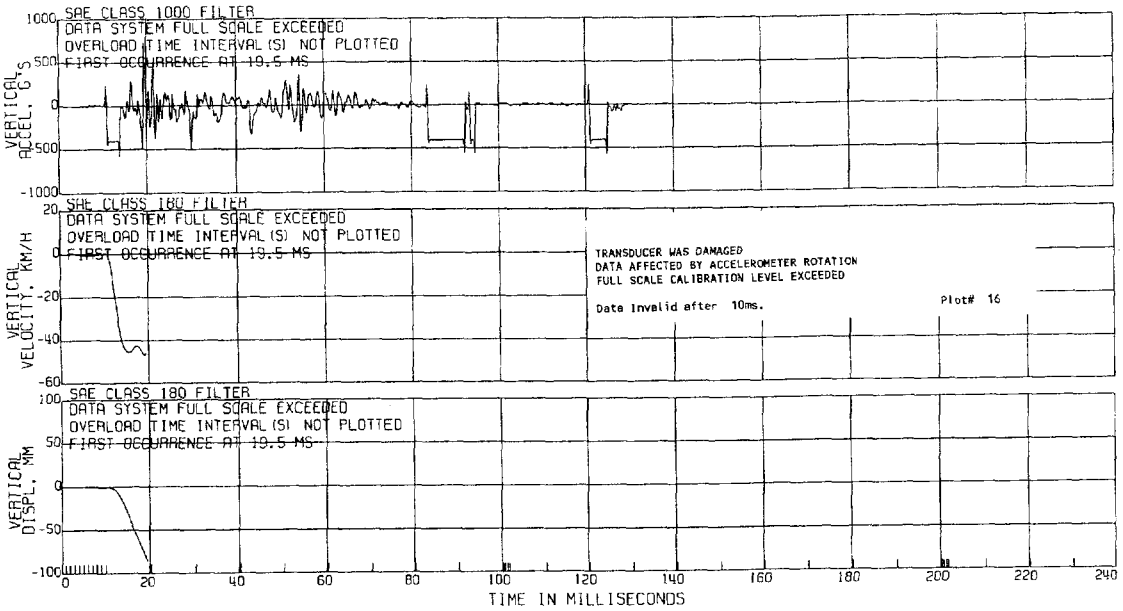

Plot A15. Crash Test C12610. Plots of acceleration, velocity, and displacement in the direction of the vertical-axis calculated from the accelerometer on the hood.

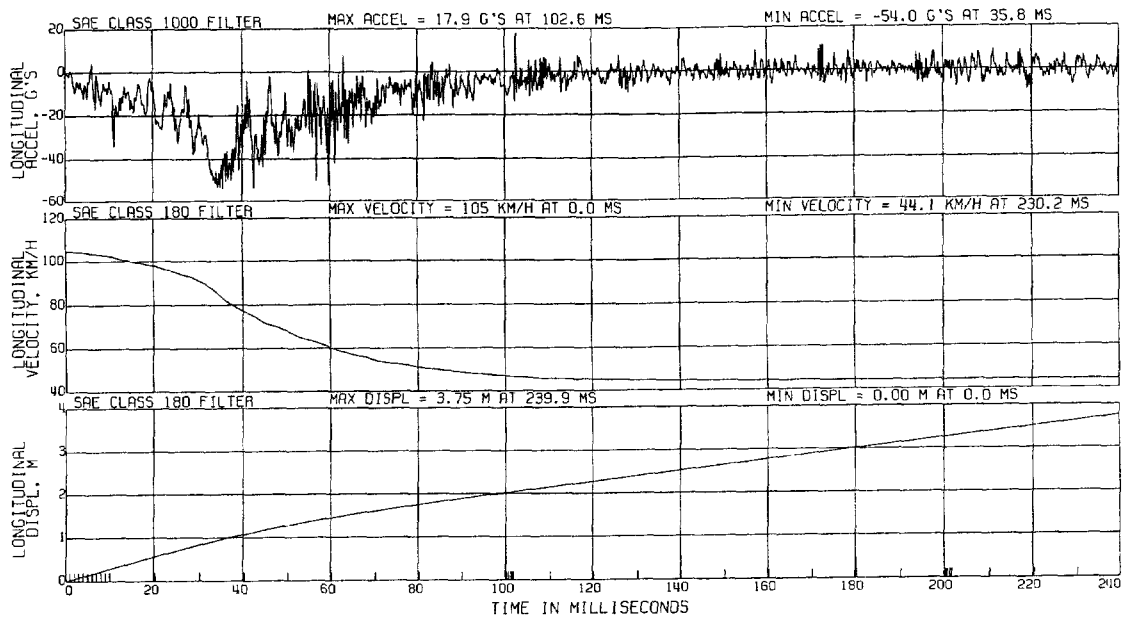

Plot A16. Crash Test C12610. Plots of acceleration, velocity, and displacement in the direction of the longitudinal-axis calculated from the accelerometer at Center of Mass on the AMDB.

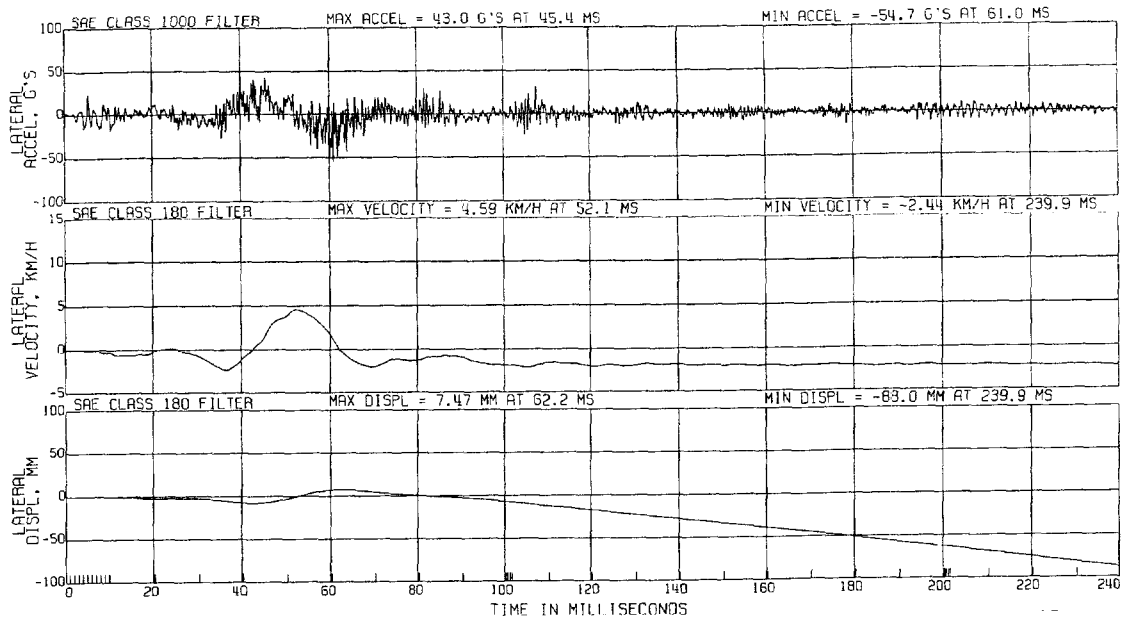

Plot A17. Crash Test C12610. Plots of acceleration, velocity, and displacement in the direction of the lateral-axis calculated from the accelerometer at Center of Mass on the AMDB.

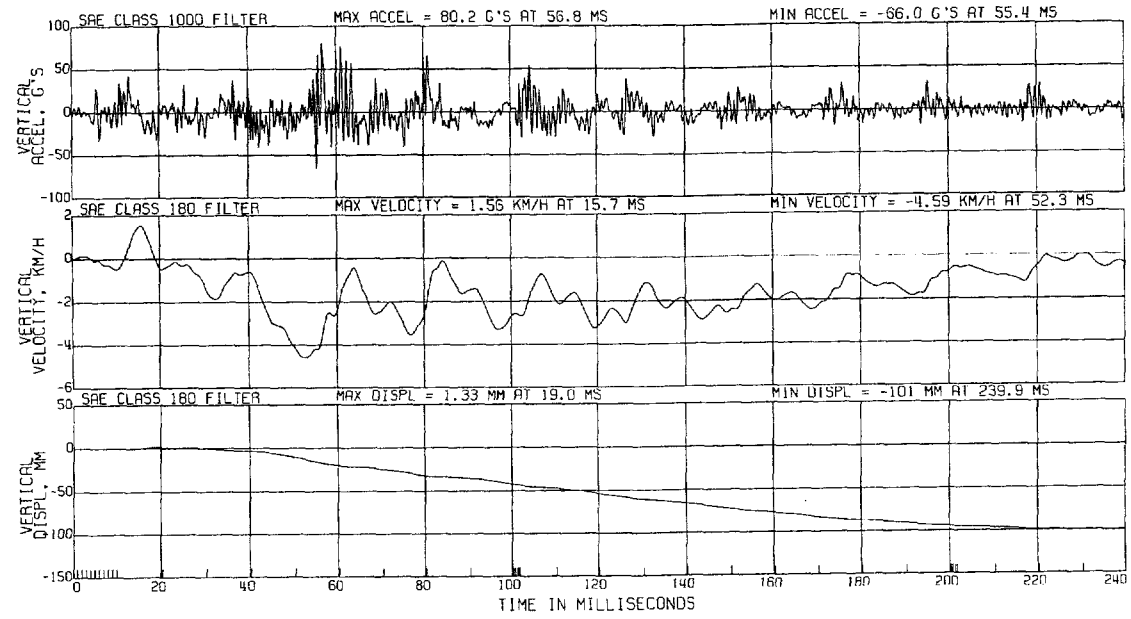

Plot A18. Crash Test C12610. Plots of acceleration, velocity, and displacement in the direction of the vertical-axis calculated from the accelerometer at Center of Mass on the AMDB.

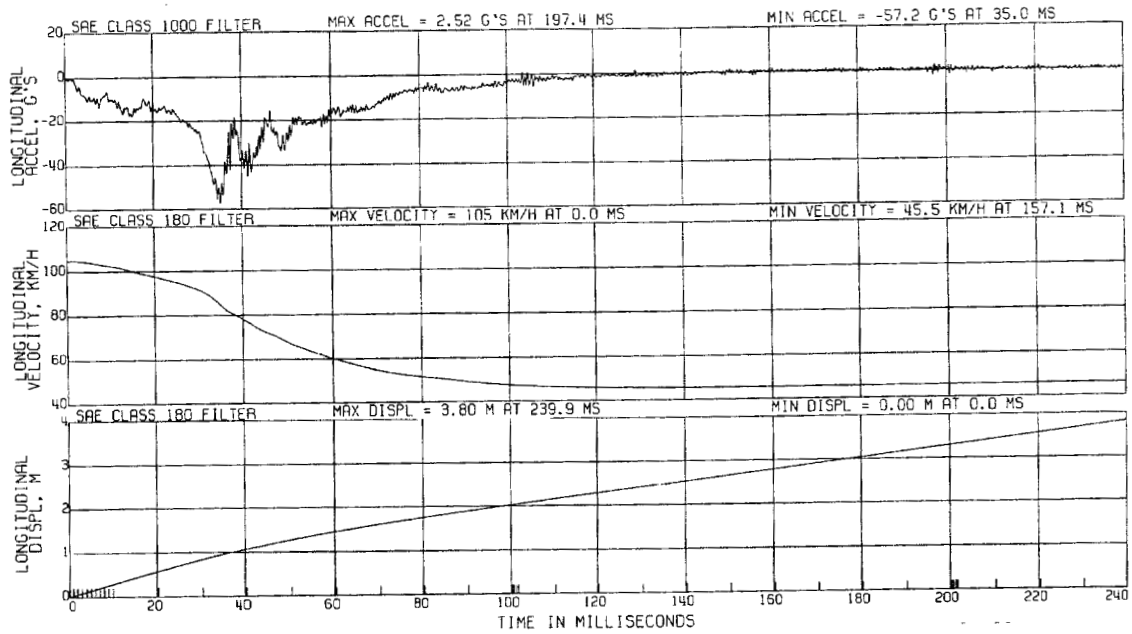

Plot A19. Crash Test C12610. Plots of acceleration, velocity, and displacement in the direction of the longitudinal-axis calculated from the accelerometer on the rear cross member on the AMDB.

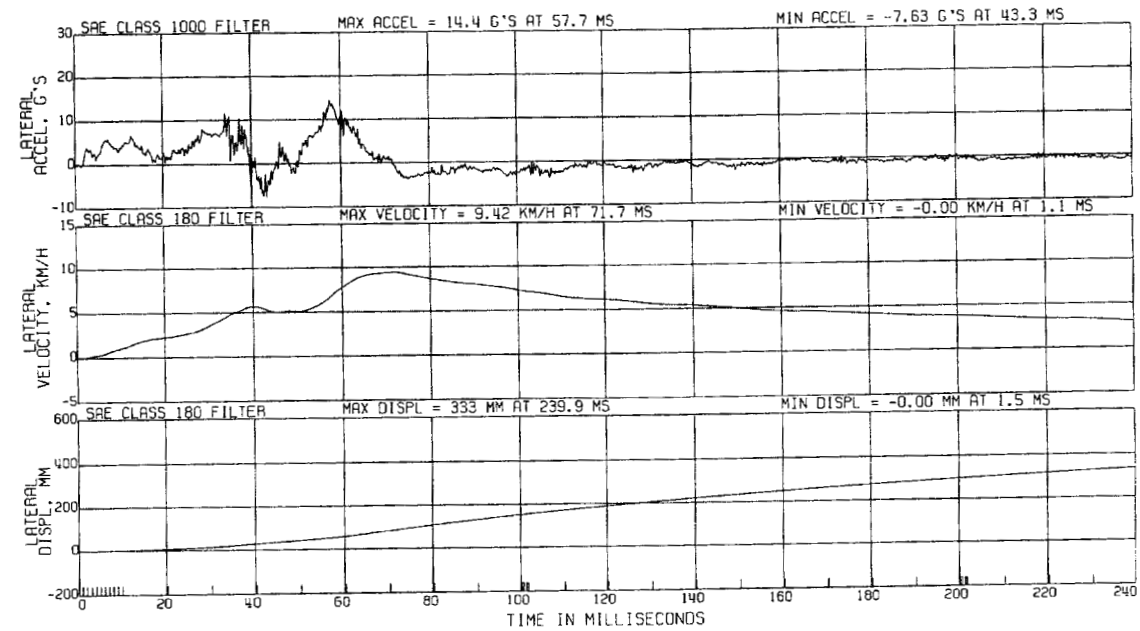

Plot A20. Crash Test C12610. Plots of acceleration, velocity, and displacement in the direction of the lateral-axis calculated from the accelerometer on the rear cross member on the AMDB.

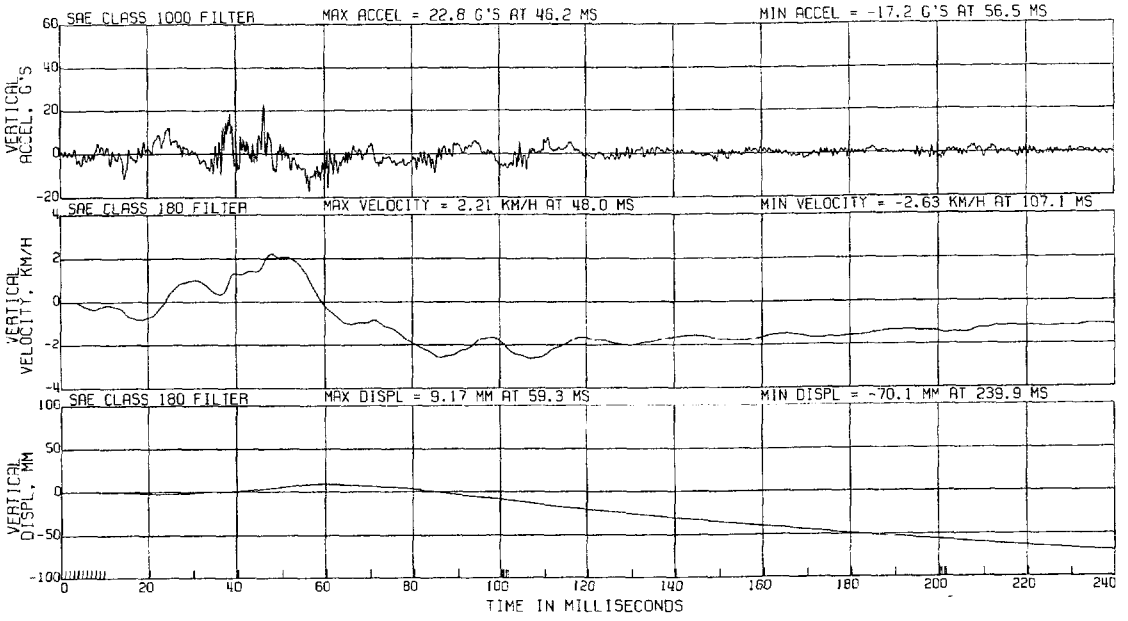

Plot A21. Crash Test C12610. Plots of acceleration, velocity, and displacement in the direction of the Vertical-axis calculated from the accelerometer on the rear cross member on the AMDB.

Appendix B

Flammable Vapor Sensor Data

Crash Test C12610

Five flammable gas sensors (TGS 813, FIGARO USA, Inc, Wilmette, IL) were installed in the engine compartments of the test vehicle. Figure B1 is a photograph of the engine compartment of the test vehicle before the crash test showing that shows the locations of the gas sensors.

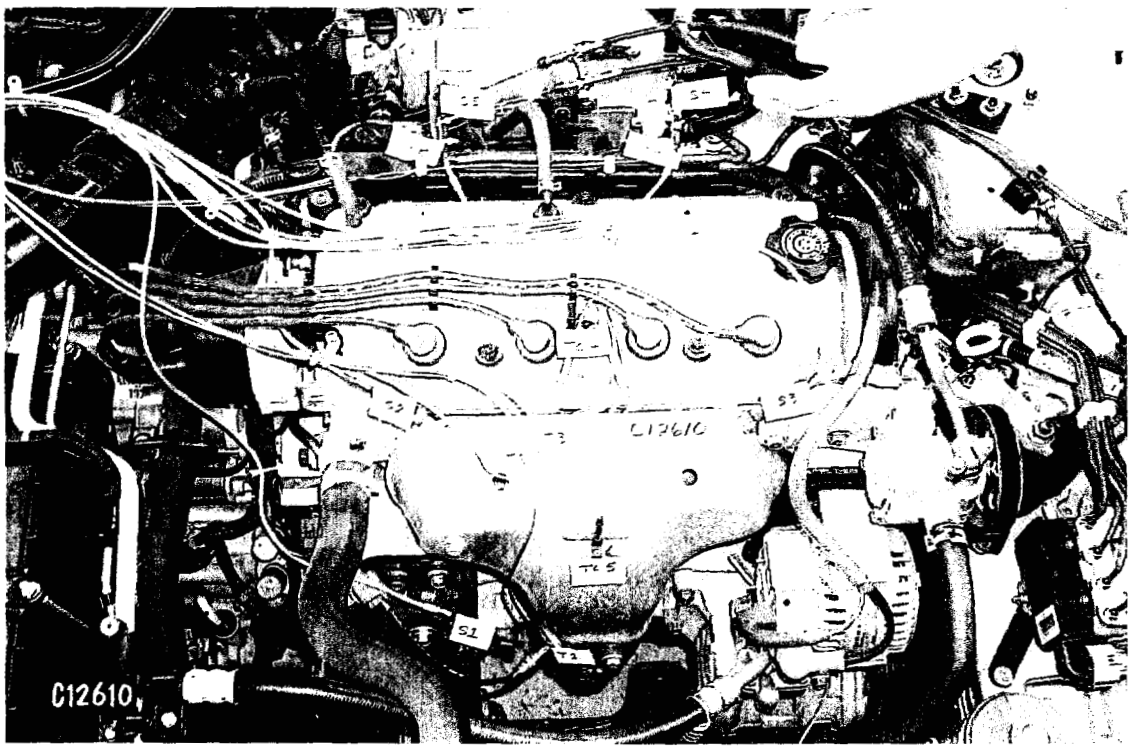

Figure B1. Crash Test C12610. Photograph of the engine compartment of the test vehicle before this crash test.

Gas Sensor S1 was located to the right of the oxygen sensor in the exhaust manifold. Gas Sensor S2 was located at the upper right of the exhaust manifold heat shield. Gas Sensor S3 was located at the upper left of the exhaust manifold heat shield. Gas Sensor S4 was located above the left side of the fuel rail. Gas Sensor S5 was located above the right side of the fuel rail.

The tin oxide semiconductor elements in these sensors also respond to changes in temperature. Exposure to heated vapor or aerosol from fluids expelled during the crash test or to the effluent from the solid propellant gas generators that activated during this test will cause the sensor output voltage to increase, which is the same response that would be expected if the sensor was

exposed to a flammable gas. It is not known to what extent these sensors were effected by exposure to the effluent from the SPGGs, which activated at approximately 300 milliseconds after time-zero. Plots B1 through B5 show plots of voltages recorded from Sensors 1 through 5, respectively. Flammable vapor concentrations were not calculated because of likely interference from the SPGG effluent.

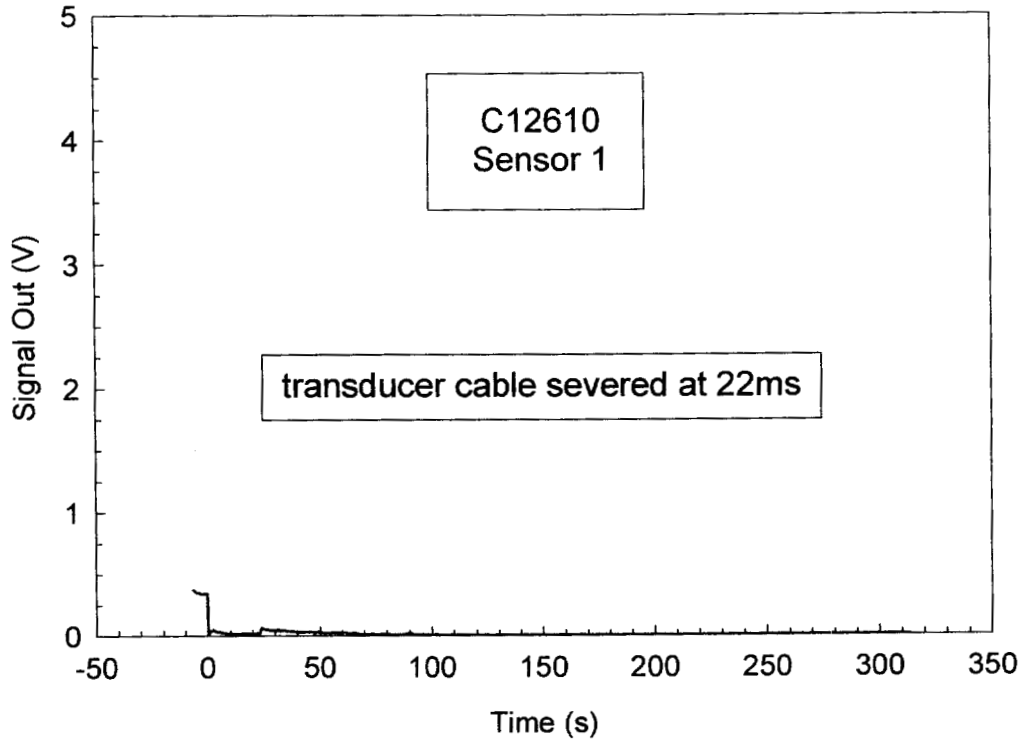

Plot B1. Crash Test C12610. Plot of voltage recorded from flammable gas sensor at Location 1.

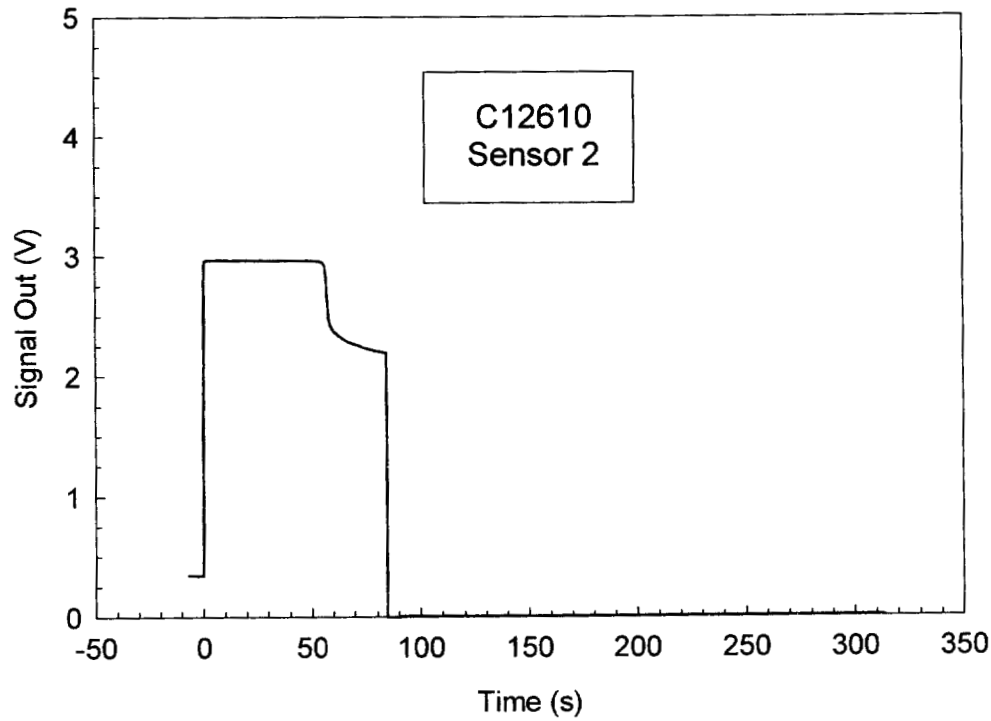

Plot B2. Crash Test C12610. Plot of voltage recorded from the flammable gas sensor at Location 2.

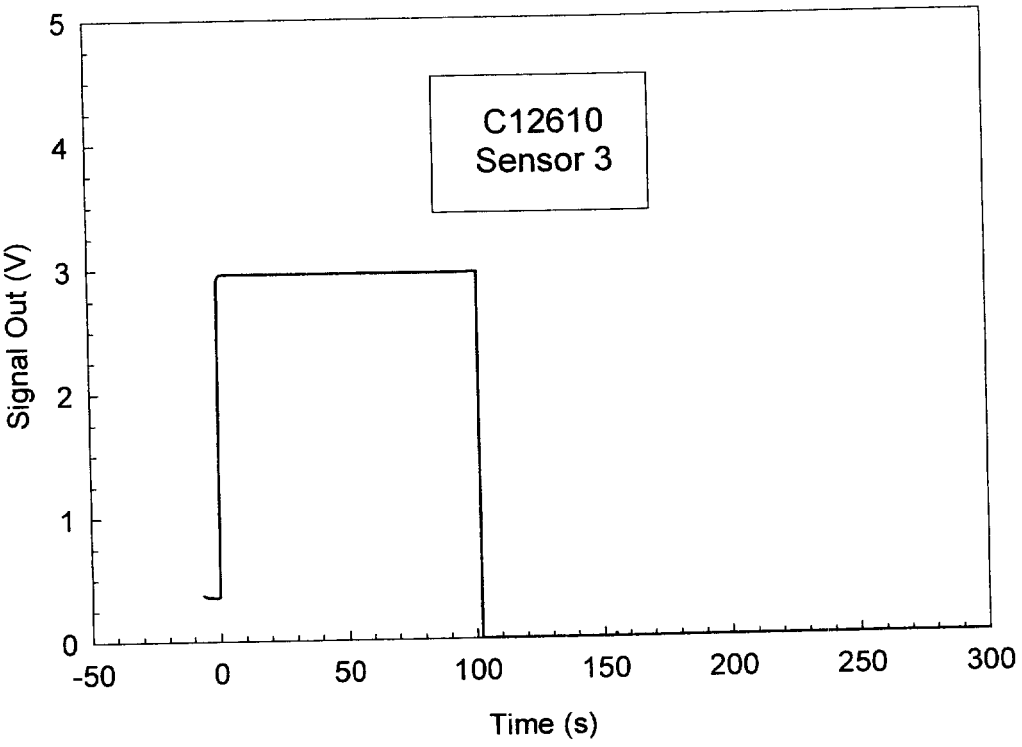

Plot B3. Crash Test C12610. Plot of voltage recorded from the flammable gas sensor at Location 3.

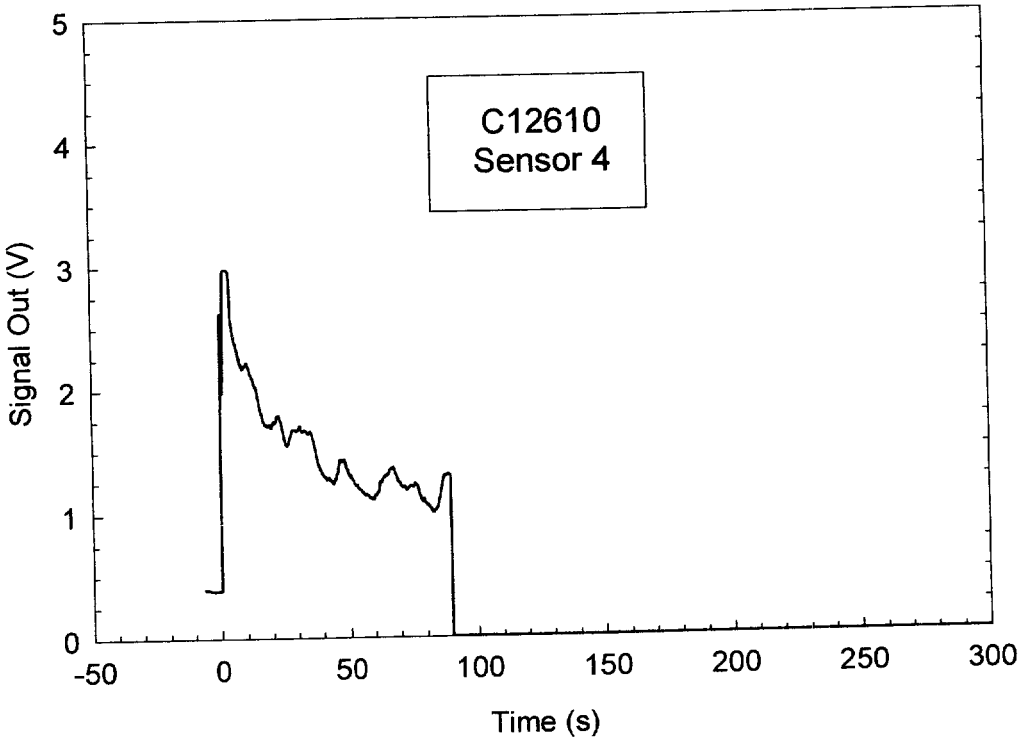

Plot B4. Crash Test C12610. Plot of voltage recorded from the flammable gas sensor at Location 4.

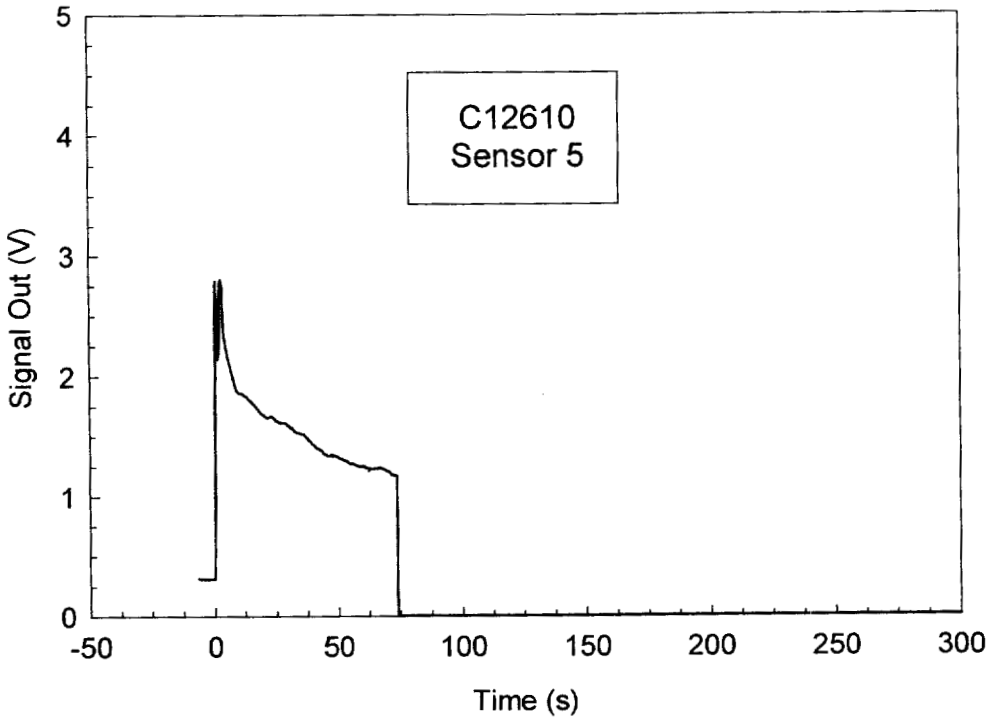

Plot B5. Crash Test C12610. Plot of voltage recorded from the flammable gas sensor at Location 5.

Appendix C

Gas Chromatography / Mass Spectroscopy Data

Crash Test C12610

Air was samples from were acquired from five locations in the engine compartments of the test vehicles during this crash test. Sample cartridges packed with an absorbent media were connected to a pumping manifold located in the rear compartments of the test vehicle. A sample cartridge consisted of a glass-lined stainless steel tube (i.d. = 4 mm; length = 10 cm; Scientific Instrument Services, Inc, Ringoes, NJ) packed with 25 mg of Carbotrap™ C Graphitized Carbon Black (Supelco, Inc.; Bellefonte, PA) in series with 15 mg of Carbotrap™ Graphitized Carbon Black (Supelco). The inlet of each sample cartridge was connected to a stainless-steel tube (o.d. = 0.125 in. (3.18 mm), i.d. = 0.085 in. (2.16 mm)), which ran from the rear compartment into the engine compartment.

The locations of the inlets to the sample tubes are shown in Figure B1. The inlet of Sample Tube T1 was located in an opening in the exhaust manifold heat shield for the oxygen sensor (Fig. B1). The inlet of Sample Tube T2 was located in the space between the top of the exhaust manifold and the exhaust manifold heat shield (Fig. B1). The inlet of Sample Tube T3 was located on the upper surface of the exhaust manifold heat shield approximately above the inlet to Sample Tube T2 (Fig. B1). The inlet of Sample Tube T4 was located in the center of the left side of the fuel rail (Fig. B1). The inlet of Sample Tube T5 was located above the right side of the fuel rail (Fig. B1).

The airflow rate through each cartridge was adjusted to 250 cm^3/min with rotometers mounted to the pumping manifold. Blank samples were acquired for a 10 minute period during the engine warm-up before the crash test. Samples during the crash test were acquired for a 15 minute period starting approximately 5 minutes before impact and ending approximately 10 minutes after impact.

Organic substances retained by the absorbent media in the sample cartridges were analyzed by thermal desorption/gas chromatography/mass spectrometry after the crash tests. Deuterated standards dissolved in deuterated methanol were added to each sorbent cartridge to monitor sample recovery. A modified purge-and-trap concentrator was used for thermal desorption (Model 600 Purge-and-Trap Concentrator, CDS Analytical, Oxford, PA). The gas chromatograph was a Model 5890 Series II Plus Gas Chromatograph (Hewlet Packard, Palo Alto, CA). The mass spectrometer was a Hewlet Packard Model 5989B Mass Spectrometer (Hewlett Packard). The thermal desorption unit was interfaced directly to the split/splitless injector of the gas chromatograph through a cryo-focusing unit. The injector was operated in the split mode with a split of approximately 10 mL/min. The chromatographic column was a fused silica capillary column coated with 100% methyl silicone (HP-1 ; length = 30 m; i.d. = 0.25 mm; film thickness = 0.25 μm).

The sample was desorbed at 320°C for 10 min, and cryofocused onto the head of the chromatographic column -80°C. The temperature of the analytical column was maintained at 0°C while the sample was desorbed and cryo-focused. To start the chromatographic analysis, the cryo-focusing unit was heated ballistically to a temperature of 320°C. The column temperature was programmed from 0 to 325°C at a rate of 5°C/min. Mass spectra were obtained by scanning from m/z 40 to 600 at a rate of 1.2 scan/s.

Plots A27 through A36 show results of GC/MS analysis of the 5 blanks acquired before this test and the 5 samples acquired during and after this test. The most intense peak in these samples was octane with t_R = 19.0 in Sample 5 (Fig. A36). The ordinates (Relative Abundance) in these mass chromatograms have been normalized to the intensity of the octane peak in Sample 5. Thus, the intensity of the signals in each of these mass chromatograms are proportional to the airborne concentrations at each location.

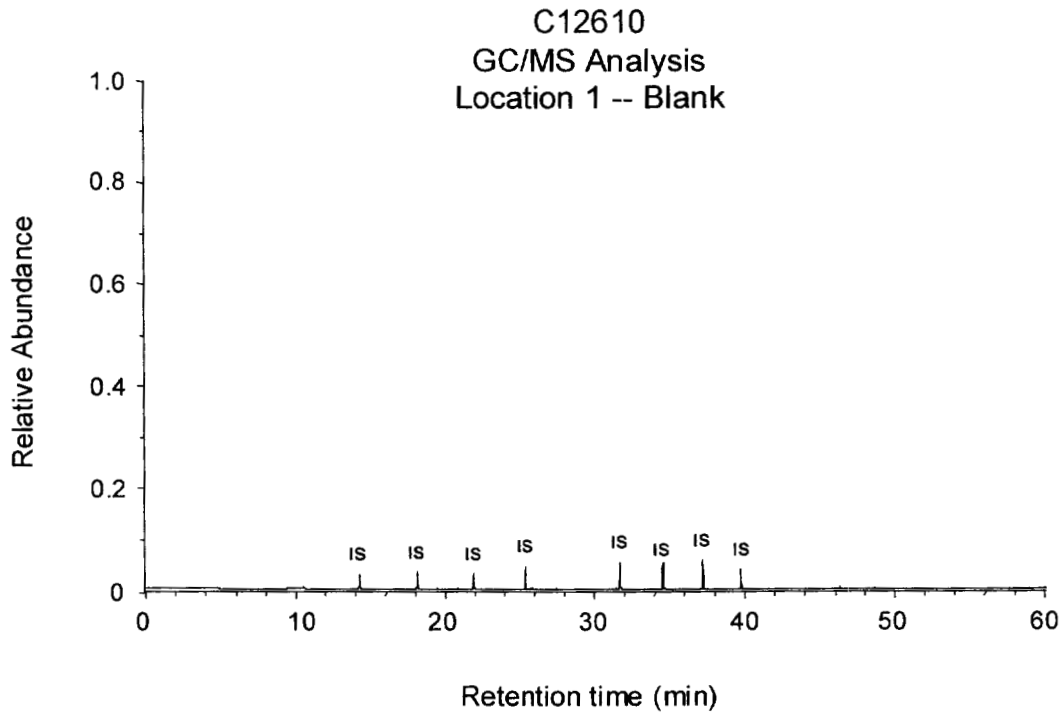

Plot C1. Crash Test C12610. Chromatogram of blank from Location 1 acquired before impact.

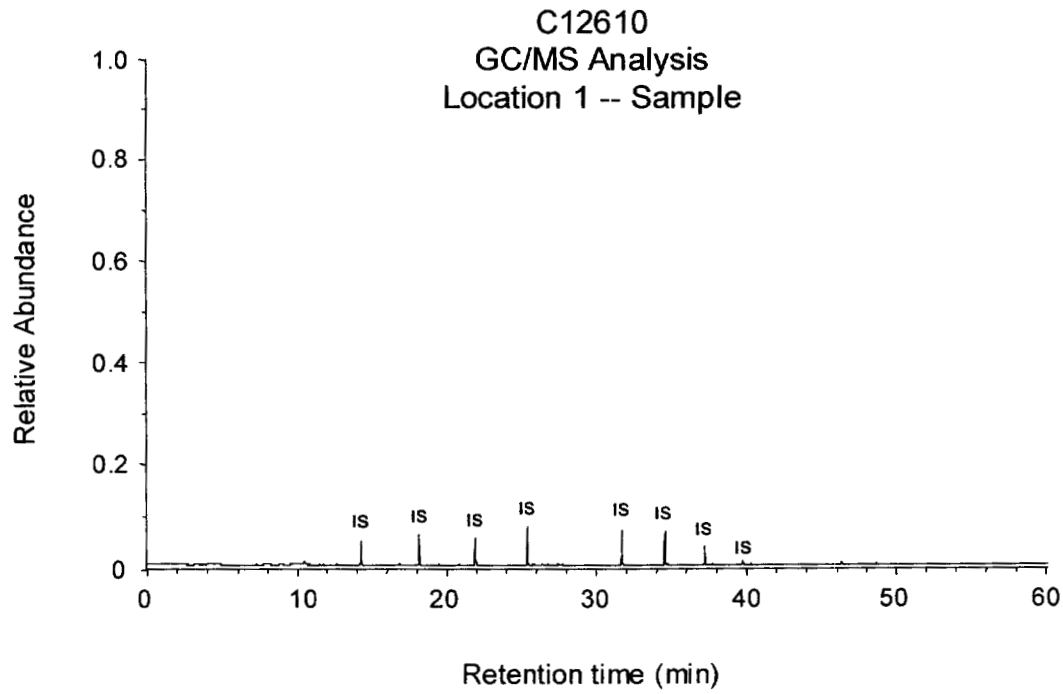

Plot C2. Crash Test C12610. Chromatogram of sample from Location 1 acquired during and after impact.

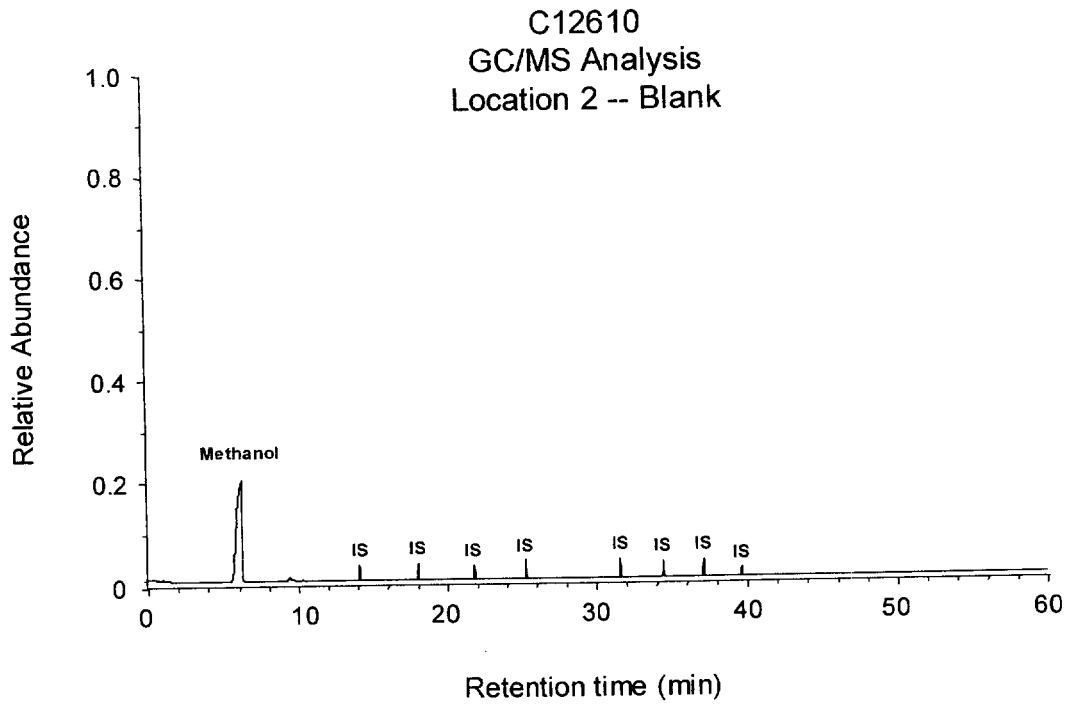

Plot C3. Crash Test C12610. Chromatogram of blank from Location 2 acquired before impact.

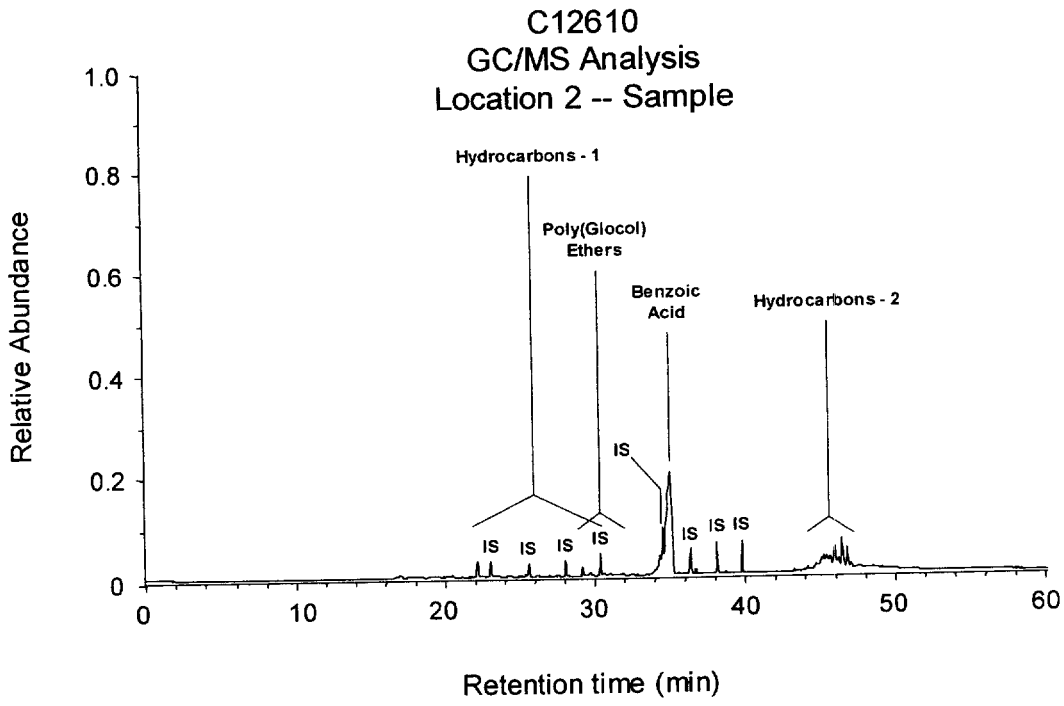

Plot C4. Crash Test C12610. Chromatogram of sample from Location 2 acquired during and after impact.

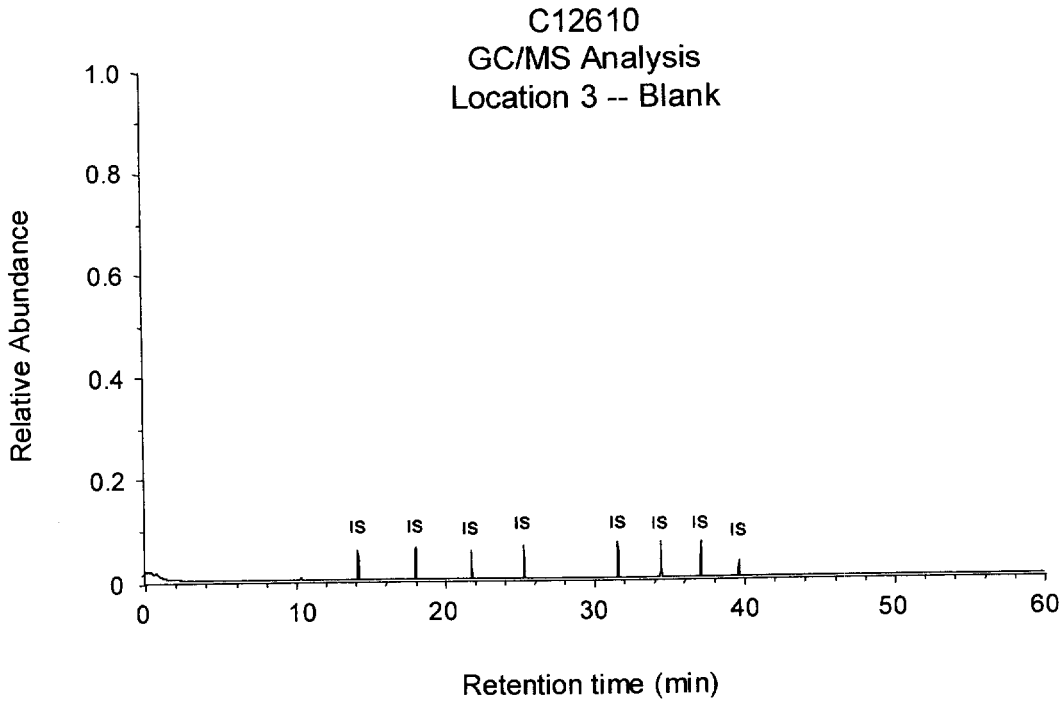

Plot C5. Crash Test C12610. Chromatogram of blank from Location 3 acquired before impact.

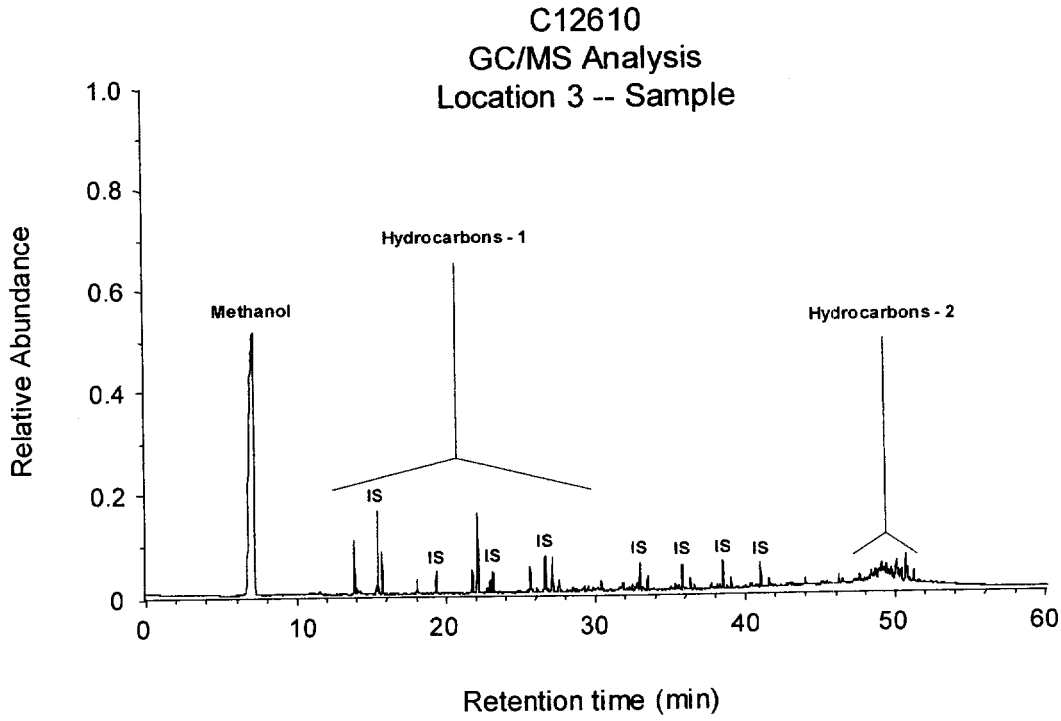

Plot C6. Crash Test C12620. Chromatogram of sample from Location 3 acquired during and after impact.

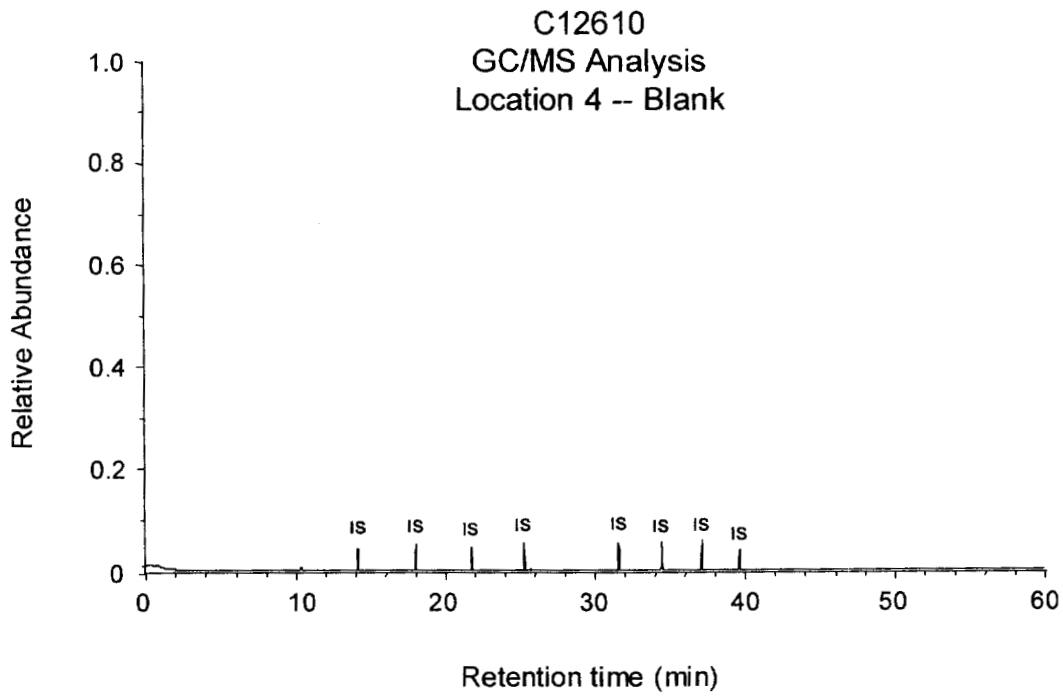

Plot C7. Crash Test C12620. Chromatogram of blank from Location 4 acquired before impact.

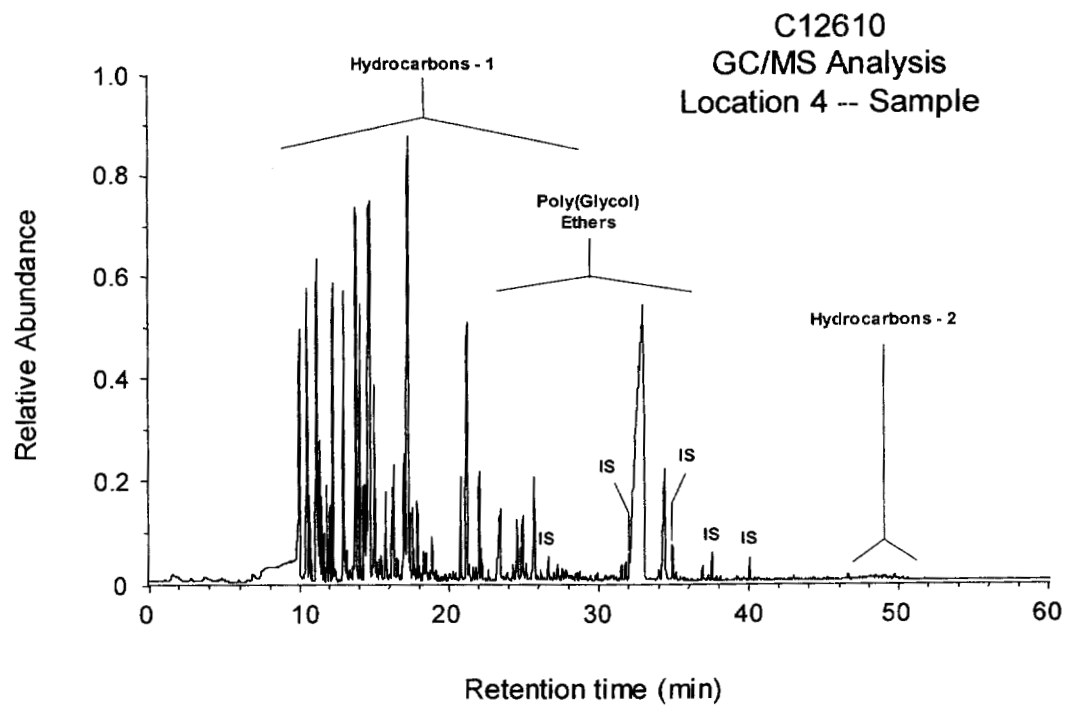

Plot C8. Crash Test C12610. Chromatogram of sample from Location 4 acquired during and after impact.

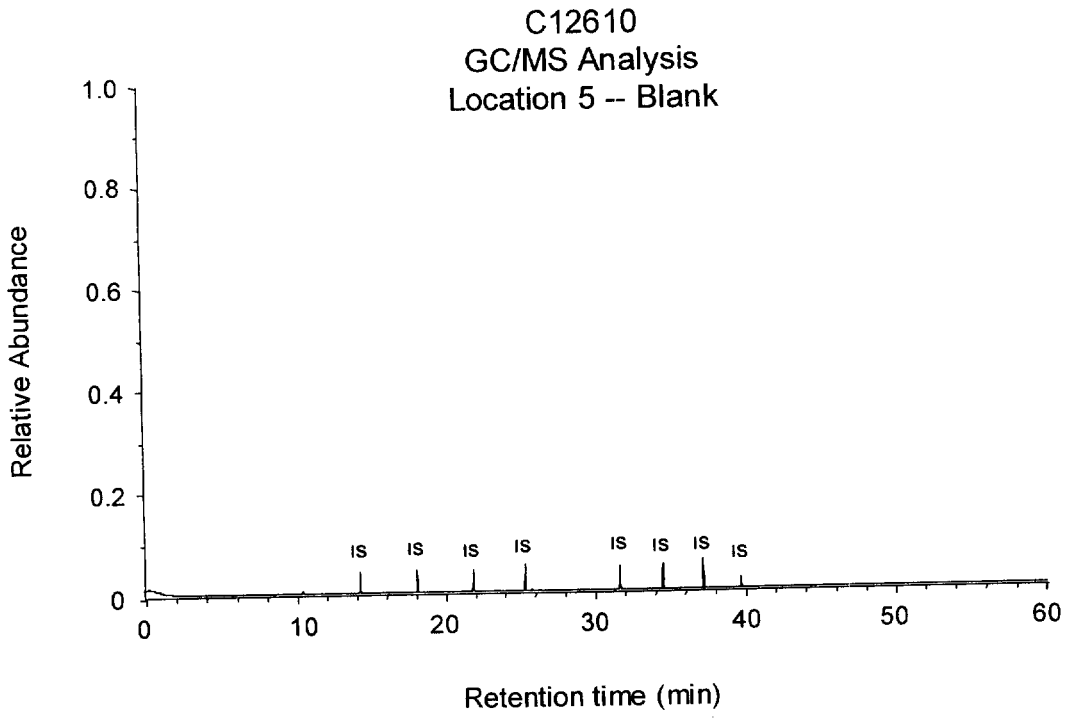

Plot C9. Crash Test C12610. Chromatogram of blank from Location 5 acquired before impact.

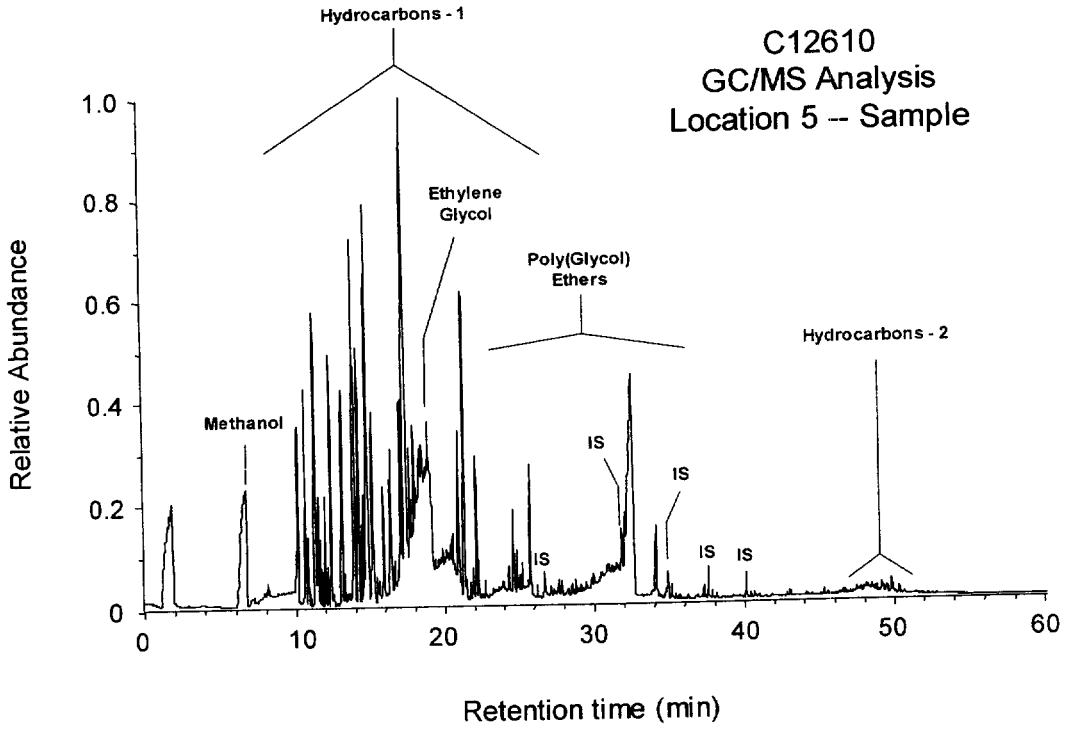

Plot C10. Crash Test C12730. Chromatogram of sample from Location 5 acquired during and after impact.

Appendix D

Component Temperature Data

Crash Test C12610

Five thermocouples were installed in the engine compartment of the test vehicle for this crash test. Figure D1 is a photograph showing the locations of Thermocouples TC1, TC2, and TC3 on the exhaust manifold of the test vehicle. Thermocouple TC1 was intrinsically welded to the runner from cylinder number 2 (Fig. D1). Thermocouple TC2 was intrinsically welded to the webbing between the runners from cylinders number 1 and 2 (Fig. D1). Thermocouple TC3 was intrinsically welded to the collector just above the oxygen sensor (Fig. D1).

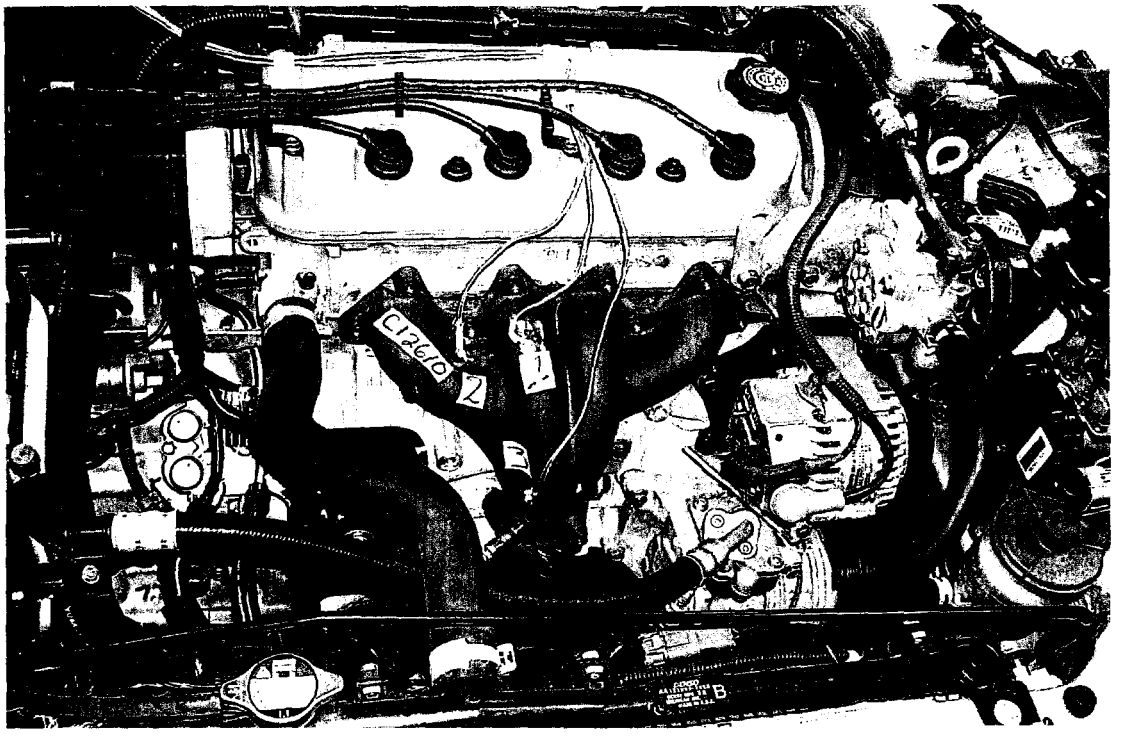

Figure D1. Crash Test C12610. Photograph showing the locations of Thermocouples TC1. TC2. and TC3 on the exhaust manifold of the test vehicle.

Figure D2 is a photograph showing the location of Thermocouple TC4 in the engine compartment of the test vehicle. Thermocouple TC4 was a shielded thermocouple located at the center of the front edge of the valve cover (Fig. D2).

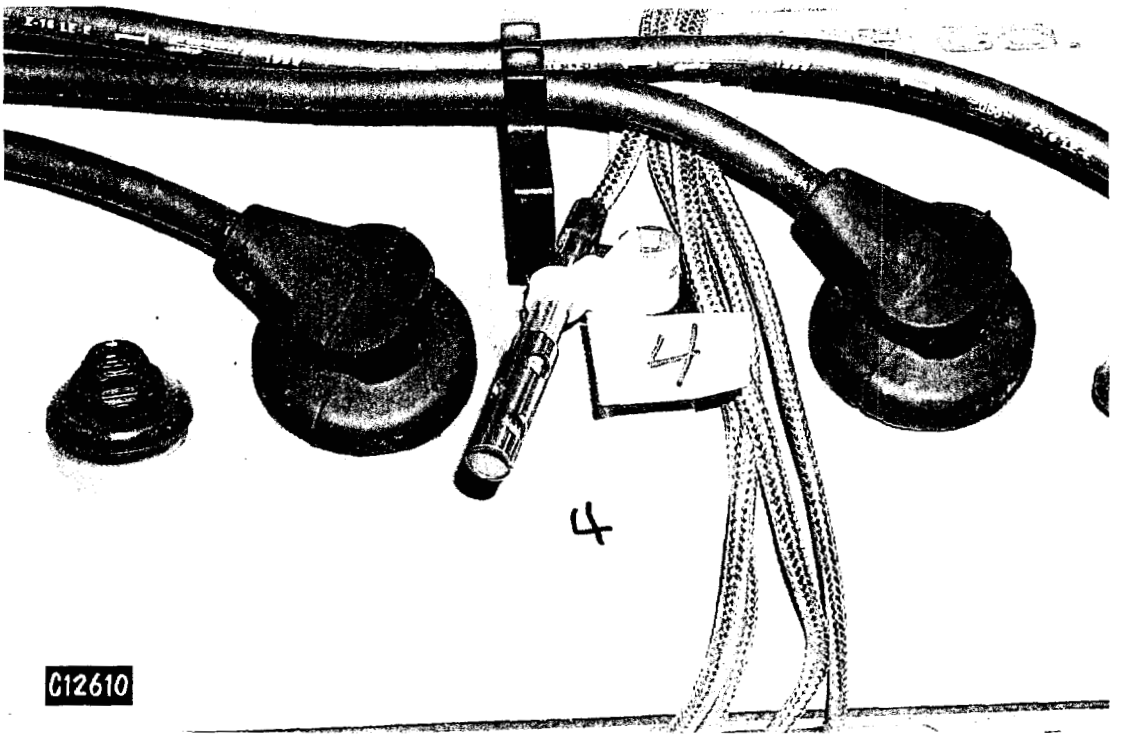

Figure D2. Crash Test C12610. Photograph showing the location of Thermocouple TC4 in the engine compartment of the test vehicle.

Figure D3 is a photograph showing the location of Thermocouple TC5 in the engine compartment of the test vehicle. Thermocouple TC5 was enclosed in a stainless steel shield pop-riveted to the outer surface of the exhaust manifold heat shield (Fig. D3).

Each thermocouple was connected to a thermocouple amplifier (OMNI-AMP IV, Omega Engineering, Stamford, CT) calibrated using a thermocouple calibrator (Model CL27, Omega) at 0, 100, 200, 300, 400, 500, 600, 700, 800, 900, and 1000°C. The output signals from the thermocouple amplifiers were recorded by the data acquisition system at the crash test facility.

Plots A37 through A40 show temperature data recorded from thermocouples TC1 through TC5, respectively. External AC electrical power to the test vehicle, and thus to the thermocouple amplifier, was turned-off 256.6 seconds after impact. Temperature data recorded after about 150 seconds post-impact were invalid because of instrumentation failure caused by the fire in the engine compartment.

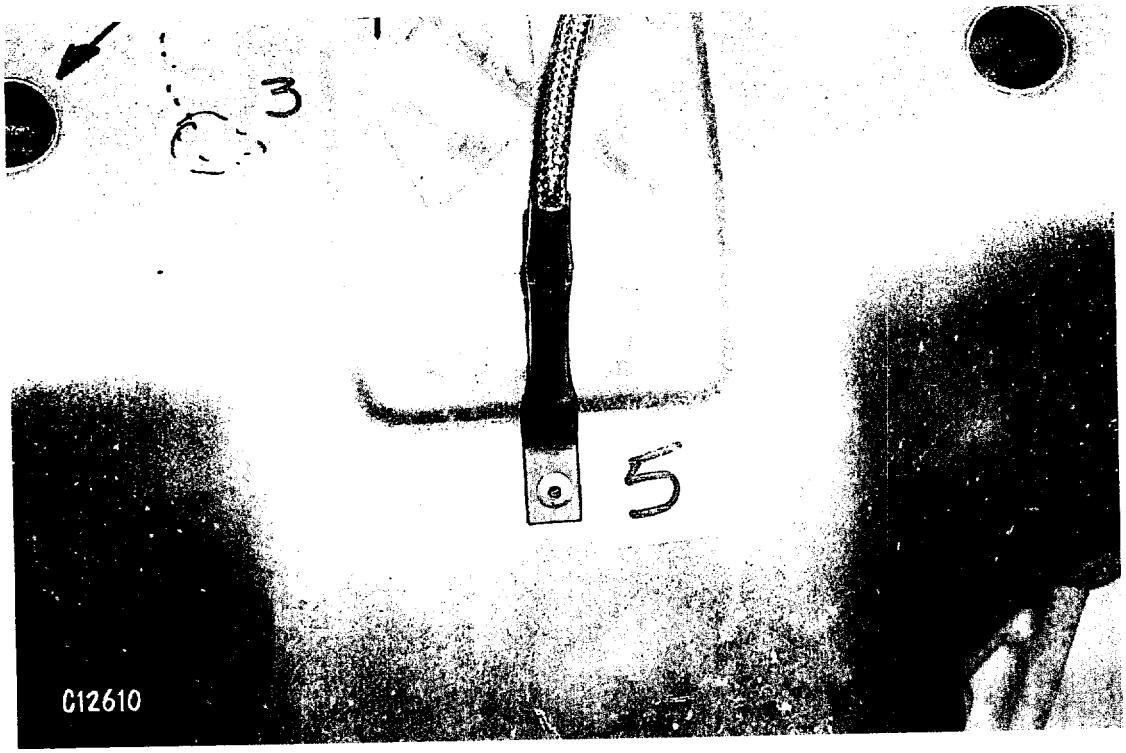

Figure A6. Crash Test C12610. Photograph showing the location of Thermocouple TC6 on the outer surface of the exhaust manifold heat shield.

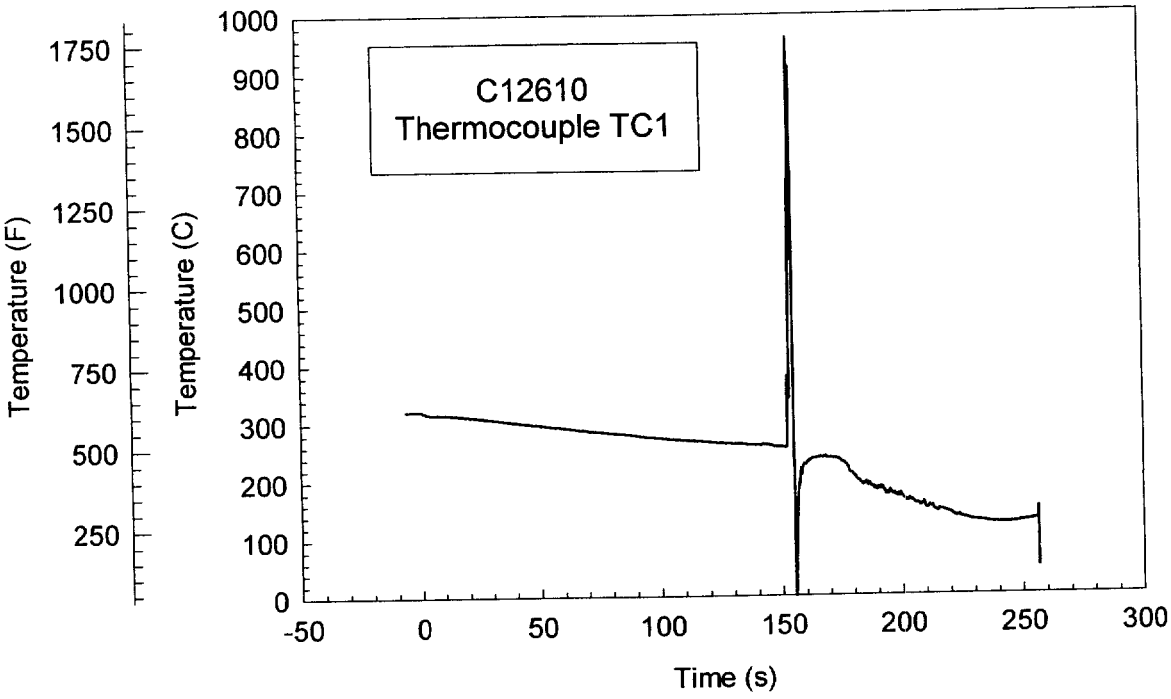

Plot D1. Crash Test C12610. Temperature data recorded from Thermocouple TC1.

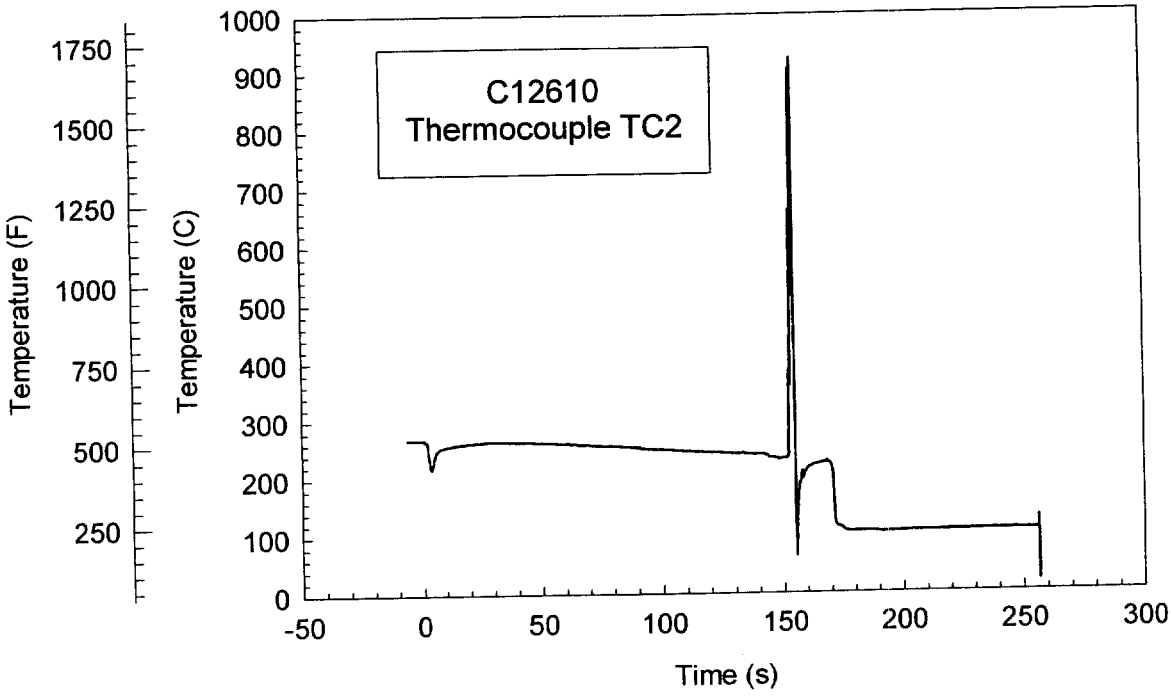

Plot D2. Crash Test C12610. Temperature data recorded from Thermocouple TC2.

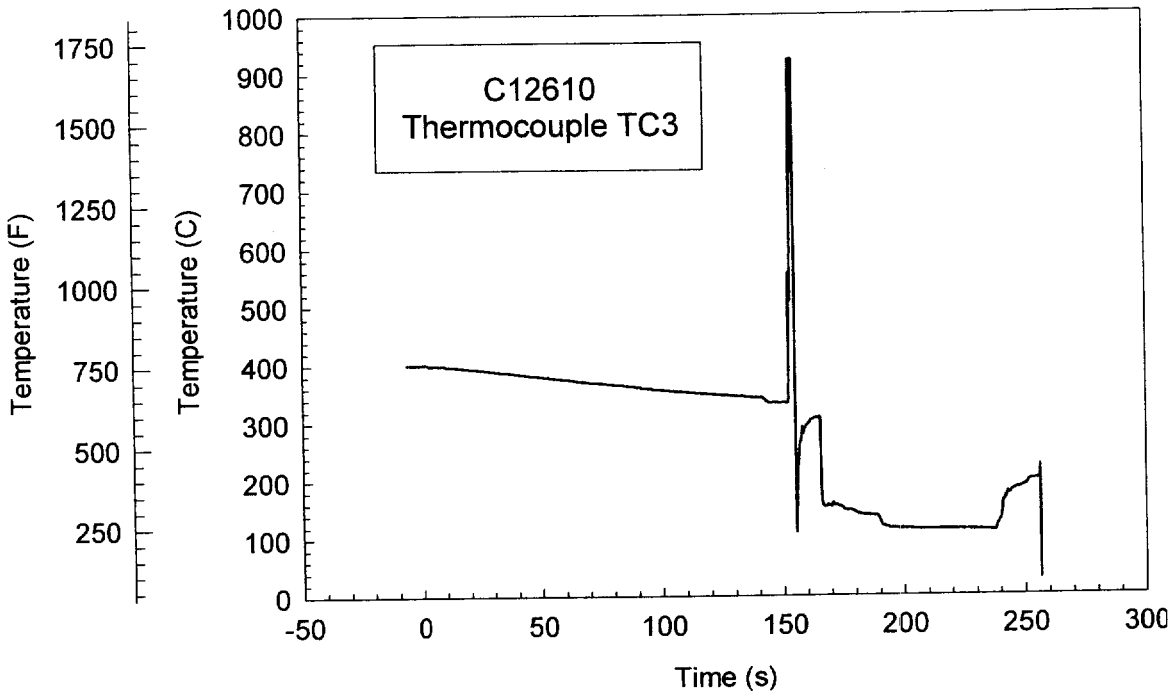

Plot D3. Crash Test C12610. Temperature data recorded from Thermocouple TC3.

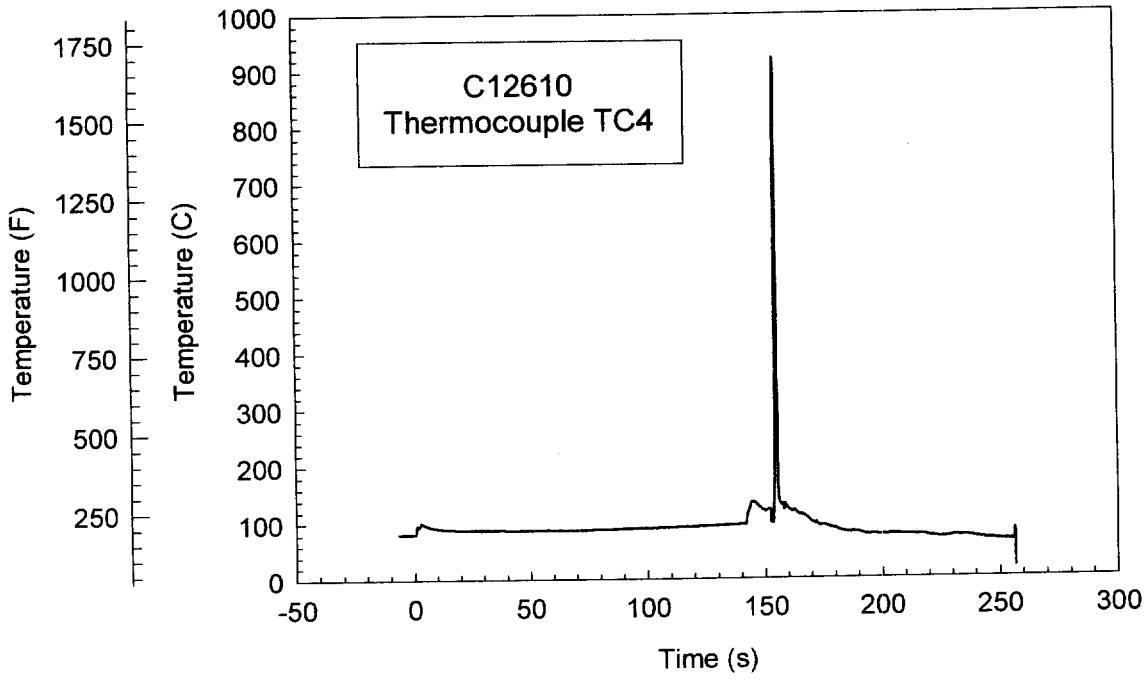

Plot D4. Crash Test C12610. Temperature data recorded from Thermocouple TC4.

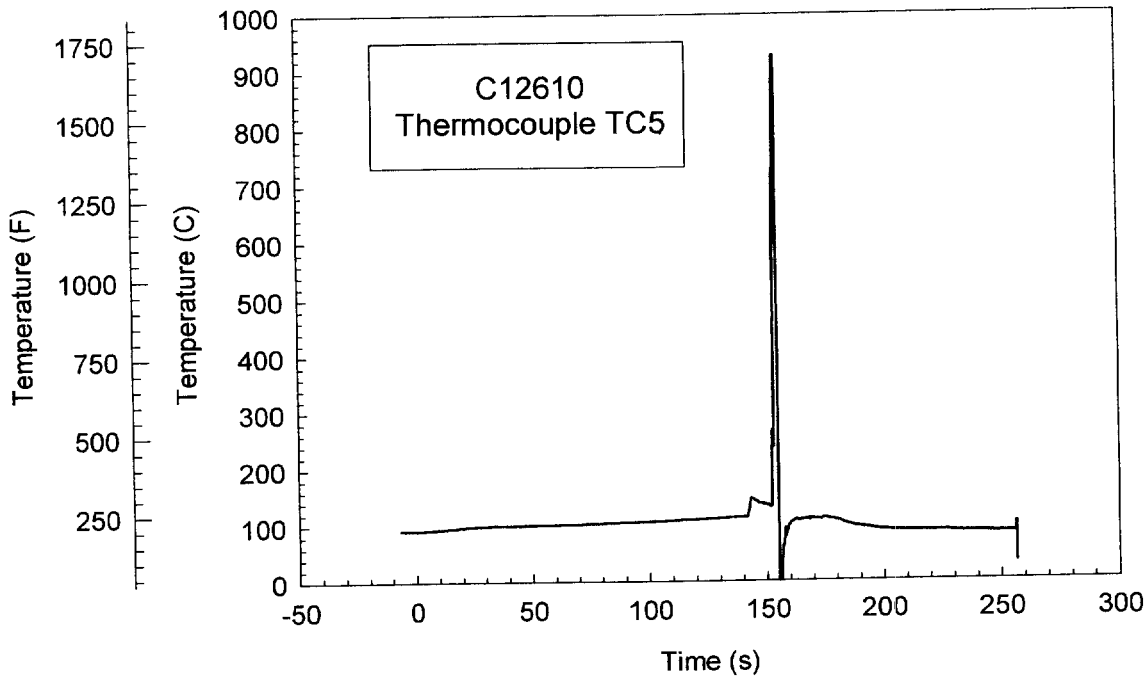

Plot D5. Crash Test C12610. Temperature data recorded from Thermocouple TC5.

Appendix E

Fire Suppression System

Crash Test C12610

The fire suppression system installed in the engine compartment of the test vehicle for this test included two prototype solid propellant gas generator fire suppression units (Atlantic Research Corporation, Knoxville, TN) and two prototype optical flame detectors (SRS Technologies, Huntsville, AL). Figure E1 is a photograph showing the locations of the solid propellant gas generator flame suppression units and optical flame detectors on the hood of the test vehicle before the crash test.

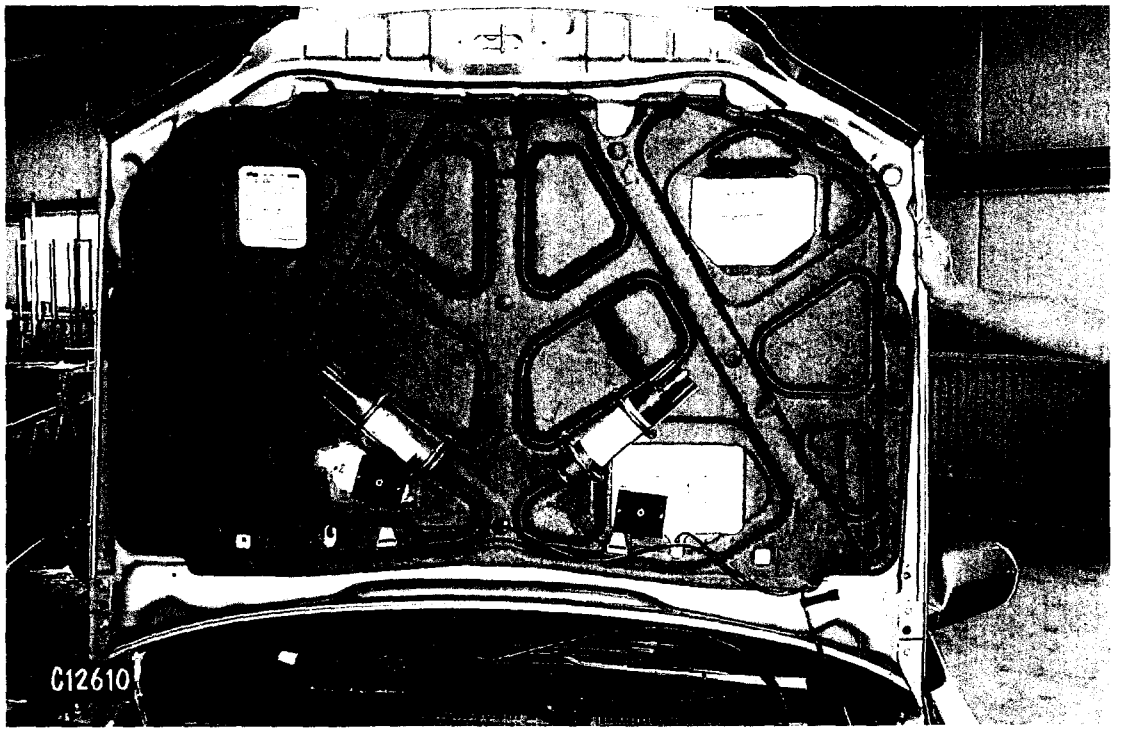

Figure E1. Crash Test C12610. Photograph showing the locations of the solid propellant gas generator flame suppression units and optical flame detectors on the hood of the test vehicle before the crash test.

The solid propellant gas generator flame suppression units were bolted to the lower surface of the hood using two U-blots for each unit (Fig. E1). The optical flame detectors were attached to the lower surface of the hood using two through-bolts for each unit (Fig. E1). Flame Suppression Unit 1 and Flame Detector 1 was attached to the left side of the hood rearward of the crush

initiator in the inner hood panel. Flame Suppression Unit 2 and Flame Detector 2 was attached to the right side of the hood rearward of the crush initiator in the inner hood panel.

Figure E2 is a wiring diagram for the flame suppression units and optical flame detectors as they were installed in the test vehicle.

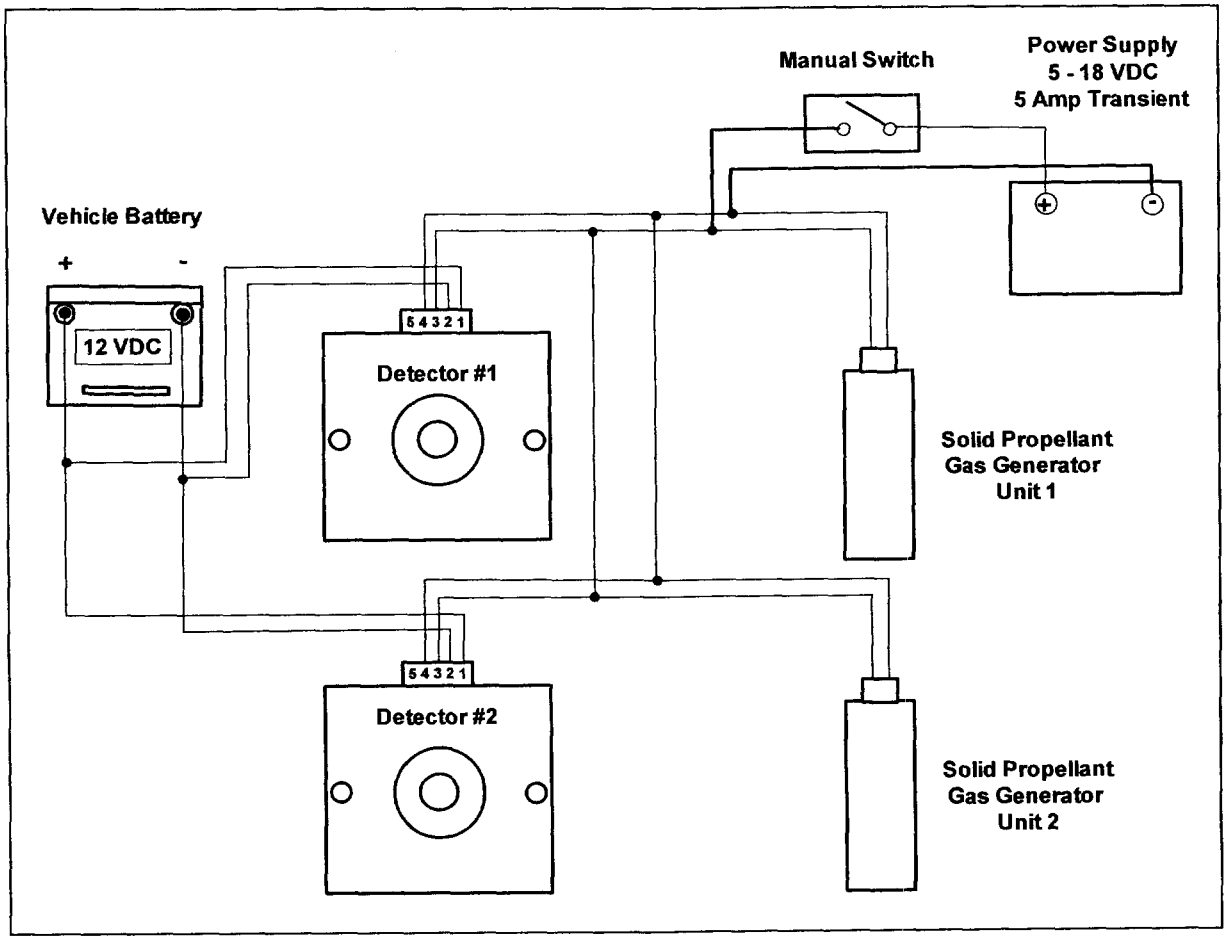

Figure E2. Crash Test C12610. Wiring schematic of the fire suppression system used in this test.

The vehicle battery supplied electrical power to the optical flame detectors. The flame suppression units were connected to the optical flame detectors in parallel so that detection of flame by either flame detector would activate both flame suppression units. A 5 to 18 VDC power supply was connected to the squib leads to the fire suppression units so that they could be activated manually during or after the crash test.

The output from each optical flame detector was monitored and recorded during this crash test. Plots E1 and E2 show the outputs recorded from these detectors from – 100 ms to + 500 ms post-impact, where the origin of the abscissa is the time of first contact between the moving barrier and the test vehicle determined by a linear contact strip on the bumper of the front test vehicle.

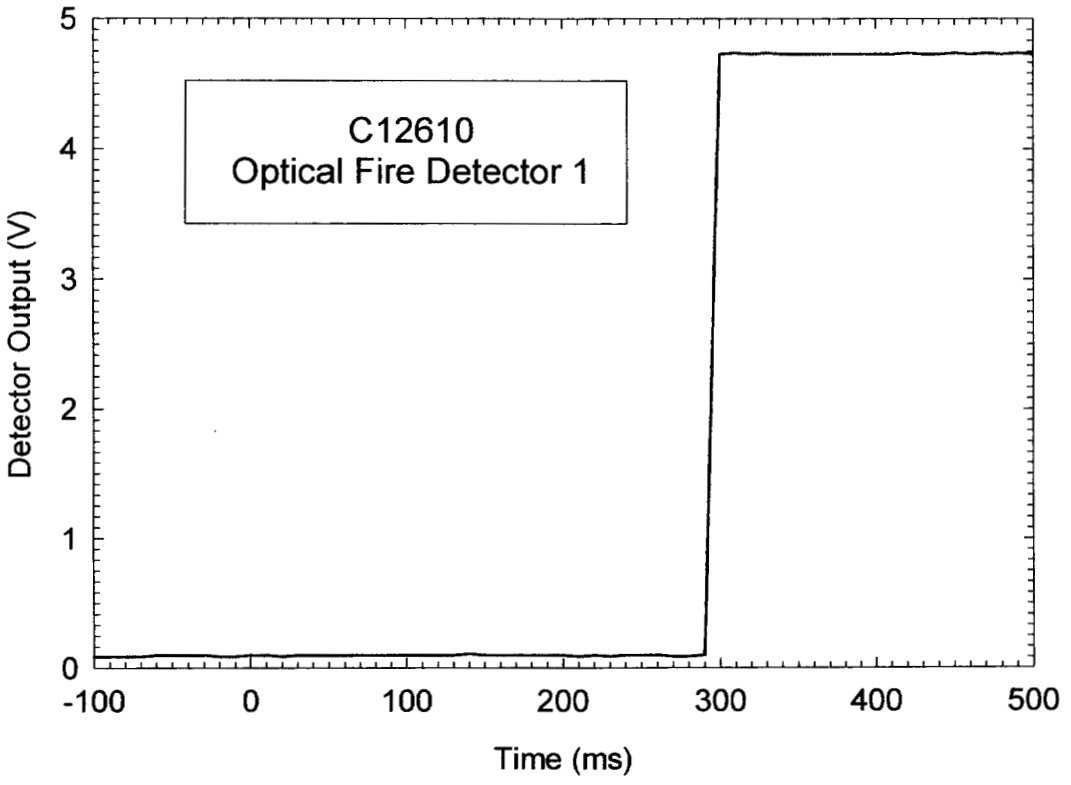

Plot E1. Crash Test C12620. Output from Optical Flame Detector 1.

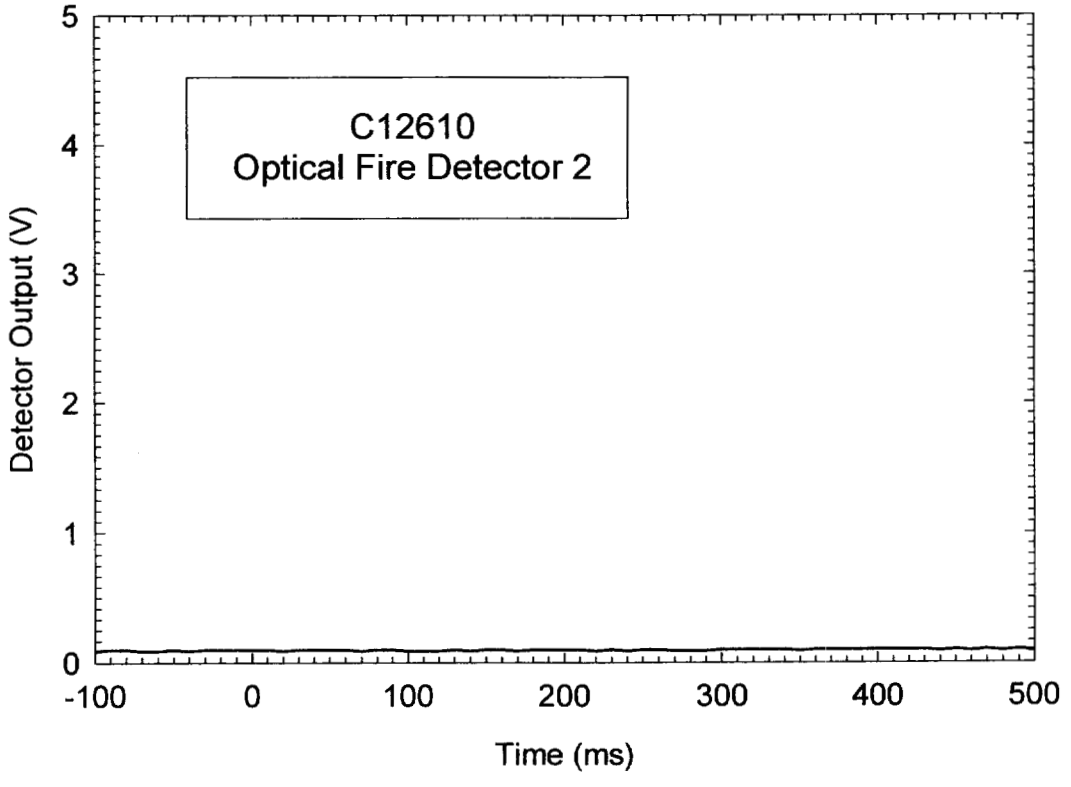

Plot E2. Crash Test C12610. Output from Optical Flame Detector 2.